

NASA CR-187117
RI/RD 87-164

1N 20
40040
P-46

FINAL REPORT

Hydrogen Test Of A Small, Low Specific Speed Centrifugal Pump Stage

by

Rocketdyne Engineering

Rocketdyne Division

Rockwell International

prepared for

NATIONAL AERONAUTICS AND SPACE ADMINISTRATION

May 1991

NASA-Lewis Research Center
Cleveland, Ohio 44135

Contract NAS3-23164

G. Paul Richter, Project Manager

(NASA-CR-187117) HYDROGEN TEST OF A SMALL,
LOW SPECIFIC SPEED CENTRIFUGAL PUMP STAGE
Final Report (Rockwell International Corp.)
46 p

N91-31213

CSCL 21H

Unclass

G3/20 0040040

Table of Contents

SUMMARY	1
INTRODUCTION	2
CONFIGURATION SELECTION & DESCRIPTION	2
TEST FACILITY DESCRIPTION	6
TEST PROGRAM	9
TEST ARTICLE	9
INSTRUMENTATION	9
TEST PROCEDURES	9
TEST MATRIX	15
TEST RESULTS	16
HEAD-FLOW	16
PUMP EFFICIENCY	20
ANALYSIS OF PUMP LOSSES	25
SUCTION PERFORMANCE	25
DIFFUSION SYSTEM PERFORMANCE	31
HYDRODYNAMIC LOADING	31
CONCLUDING REMARKS	40
REFERENCES	41

List of Figures

Figure 1 - Shrouded Impeller Volute Pump.....	5
Figure 2 - LH ₂ Test Facility Schematic.....	7
Figure 3 - Pump / Turbine Test Stand Installation.....	8
Figure 4 - Pump / Tester Cross Section.....	10
Figure 5 - Pump / Tester Assembly.....	11
Figure 6 - Typical Pump Instrumentation.....	12
Figure 7 - Tester and Turbine Instrumentation.....	13
Figure 8 - Isentropic Head Flow.....	17
Figure 9 - Low Thrust Hydrogen Test, Config. 2, H/Q Test.....	18
Figure 10 - Low-Thrust Water Testing, Config. 2.....	19
Figure 11 - Low Thrust Hydrogen Testing, Config. 2, Test 016027.....	21
Figure 12 - Low Thrust Hydrogen Test, Config. 2, Isentropic Pump Efficiency.....	22
Figure 13 - Low Thrust Turbine Efficiency.....	23
Figure 14 - Low Thrust Tester Torque, Liquid Hydrogen Lubrication.....	24
Figure 15 - Low Thrust Hydrogen Test, Config. 2.....	26
Figure 16 - Low Thrust Hydrogen Testing, CAV Test 016027.....	27
Figure 17 - Low Thrust Hydrogen Test, Config. 2, H/Q Testing.....	30
Figure 18 - Low Thrust Hydrogen Testing, Config. 2, CAV Test 016026.....	32
Figure 19 - Low Thrust Hydrogen Testing, Config. 2, CAV Test 016027.....	33
Figure 20 - Low Thrust Hydrogen Testing, Config. 2, Section Specific Speed.....	34
Figure 21 - Low Thrust Hydrogen Testing, Config. 2, Suct.Perform.for LH ₂ & H ₂ O.....	35
Figure 22 - Diffusion System, Config. 2.....	36
Figure 23 - Low Thrust Hydrogen Testing, Config. 2, Impeller Volute H/Q.....	38
Figure 24 - Low Thrust Hydrogen Testing, Config. 2, Radial Load.....	39

List of Tables

Table I - Design Summary of Centrifugal Pump Configurations.....	3
Table II - Pump Design Geometry.....	4
Table III - LH2 Centrifugal Pump Test Instrumentation List.....	14
Table IV - Instrumentation Accuracies.....	15
Table V - Test Matrix.....	15
Table VI - Predicted Design Point Losses as Percent of Input Power at Operating Wear Ring Clearances.....	28
Table VII - Design Point Pump Efficiencies	29

SUMMARY

A small, low specific speed ($430 \text{ RPM} \cdot \text{GPM}^{0.5} / \text{ft}^{0.75}$) centrifugal pump stage with a 2 inch tip diameter, 0.030 inch tip width shrouded impeller and volute collector, which had previously been tested in water, was tested with liquid hydrogen as the pumped fluid. Data in hydrogen obtained at test speeds of 60% and 80% of design speed were scaled to the 77,000 RPM design speed using appropriate affinity laws. The head / flow characteristic in hydrogen was relatively flat over the test flow range similar to the characteristic determined in the previous water tests. Based on scaled data from the 80% test speed, the pump overall isentropic head rise was 7,000 feet at design flow. Efficiency was 30.3% based on output power delivered from a calibrated drive turbine. Impeller wear ring radial clearances for the hydrogen tests were over twice the design value of 0.002 inch and significantly affected the test efficiency. Results of loss analyses using as-tested clearances indicated that an efficiency of 43.7% could be expected when operating at design clearance. Limited cavitation data indicated that the pump had better suction performance in hydrogen than in water at corresponding flow ration conditions.

INTRODUCTION

Pump-fed low-thrust chemical propulsion systems are being considered for transferring acceleration-limited structures from low earth orbit to geosynchronous or other high earth orbits. Engine systems for these applications will require small, relatively low flow rate, high head rise pumps that fall outside the design range of existing rocket engine turbopumps. In order to establish a technology base for future design of these systems, a program was initiated to experimentally evaluate low specific speed centrifugal pump stages and inlet-type stages over the flow rate range of interest. Funding for the program was provided under NASA-Lewis Research Center Contract NAS3-23164 and related effort was provided by Rocketdyne internal sources.

Contracted effort consisted of design, fabrication and water test of six single-stage centrifugal pump configurations with subsequent test of one of the configurations in liquid hydrogen. The tester and drive turbine used in the test effort were fabricated and test-calibrated as part of a prior Rocketdyne-funded program. Also, an inducer was designed and fabricated under contract and a shear force pump stage was designed and fabricated under the prior company-funded program. Because of a reduction in program scope, neither of these units was tested. The reduction in scope likewise precluded tests in liquid hydrogen of a second of the centrifugal pump stages.

Results of the water testing along with design details of the six centrifugal configurations are given in reference 1. This report presents liquid hydrogen test results of Configuration 2, a 430 (RPM*GPM** $0.5/\text{ft}^{0.75}$) design specific speed stage with a 100% admission shrouded impeller discharging directly into a volute.

CONFIGURATION SELECTION & DESCRIPTION

A complete description of the six centrifugal pump configurations along with their performance characteristics in water are given in reference 1. A design summary of the configurations is given in Table I. Following the water tests, the performance and design advantages of the six configurations were evaluated by NASA Lewis Research Center and Rocketdyne with Configuration 2 chosen as the first of two configurations to be tested in liquid hydrogen. Configuration 6 which included a shrouded impeller with a 0.052 inch tip width (for ease of fabrication) and a 50% emission vaned diffuser was selected as the second configuration but was not tested because of the previously noted reduction in program scope.

Design details for Configuration 2 are given in Table II. Pump hardware is shown in Figure 1. The pump incorporates a 100% admission full shrouded 2-inch tip diameter impeller with seven backwardly curved blades which have a 33 degree discharge blade angle. Impeller discharge tip width is 0.030 inch. Impeller flow discharges directly into a volute with a diffusion section at the exit.

Table I - Design Summary of Centrifugal Pump Configurations

Configuration	Impeller		Tip Width, Inches	Diffuser Type	Fluid	Speed, RPM	Flow, GPM	Head, Feet	Specific Speed, RPM rpm* ^{0.5} gpm /ft ^{0.75}
	Type	Discharge Diameter Inches							
1	Shrouded 100% Admission	2.00	0.030	Vaned 100% Emission	Water Hydrogen	24,500 77,000	5.0 15.7	637 6,300	430 430
2	Same as Configuration 1	2.00	0.030	Volute Exit	Water Hydrogen	24,500 77,000	5.0 15.7	637 6,300	430 430
3	Same as Configuration 1	2.00	0.030	Vaned 25% Emission	Water Hydrogen	39,200 125,000	2.0 6.3	1,630 16,600	215 215
4	Open Face 100% Admission	2.00	0.035	Volute Exit	Water Hydrogen	24,500 77,000	5.0 15.7	637 6,300	430 430
5	Open Face 25% Admission	2.00	0.035	Volute Exit	Water Hydrogen	39,200 125,000	2.0 6.7	1,711 17,400	215 215
6	Shrouded 100% Admission	2.00	0.052	Vaned 50% Emission	Water Hydrogen	24,500 77,000	5.0 15.7	637 6,300	430 430

Table II - Pump Design Geometry
Configuration NO. 2

Impeller

<u>Type</u>	<u>Shrouded</u>
Discharge diameter, inches	2.0
Inlet Eye diameter, inches	0.75
Inlet Hub diameter, inches	0.50
Discharge tip width, inches	0.030
Number of Blades	7
Discharge Blade angle, degrees	33
Wear Ring diameter, inches	1.00
Front Wear Ring Radial clearance Inches (maximum design)	0.002
Impeller Face clearance, inches	----
Rear Wear Ring radial clearance Inches (maximum design)	0.002
Inlet Eye Blade angle, degrees	21.9
Inlet flow coefficient (10% blockage)	0.134
Percent admission	100
Discharge Flow coefficient	0.074

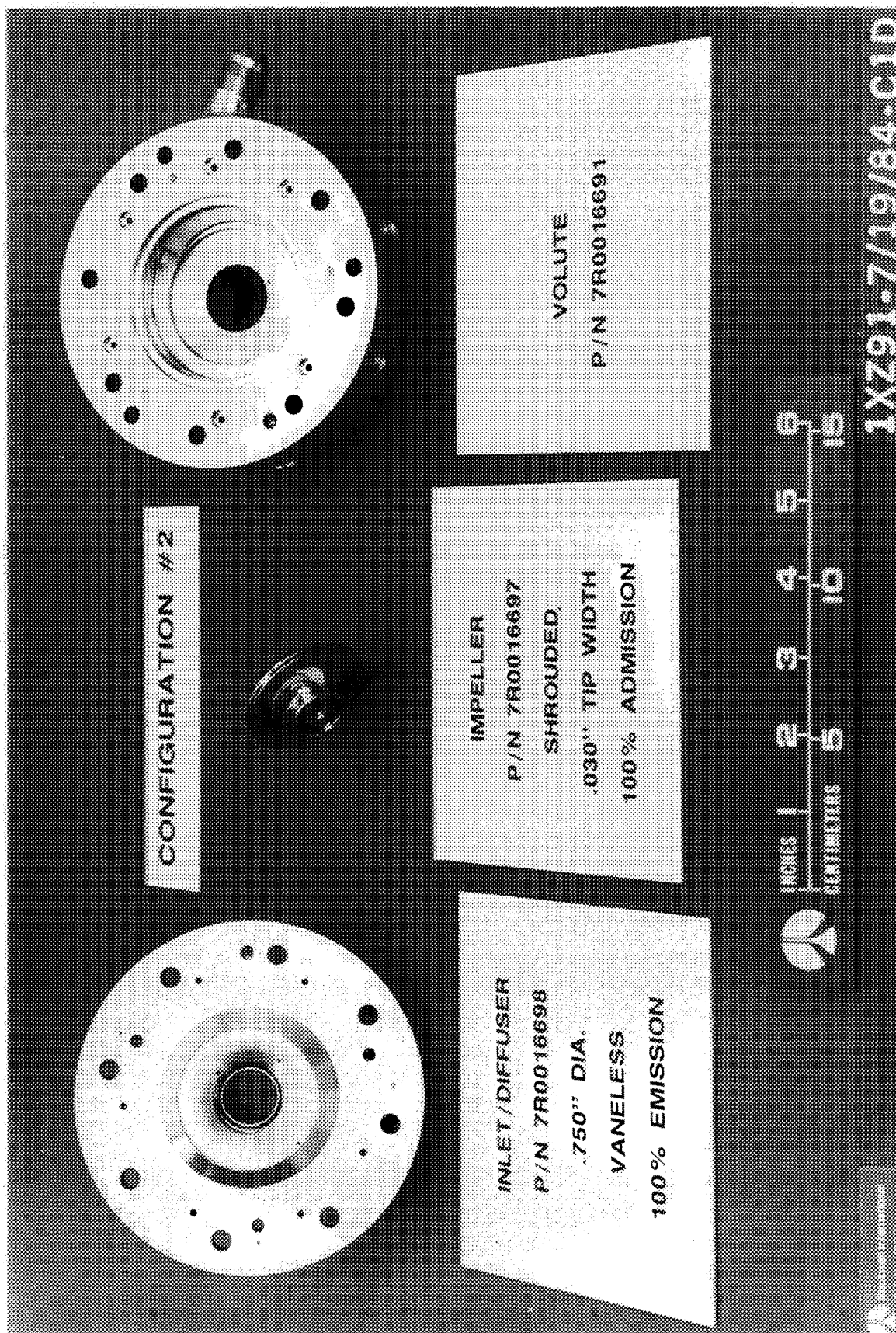
Diffuser

Inlet diameter, inches	----
Discharge diameter inches	----
Passage width, inches	----
Number of passages	----
Inlet angle, degrees	----
Area ratio, out/in	----
Percent emission	----

Volute

Maximum area at 360 degrees, in. ²	0.0267
Continuity area/Actual area	0.60
Conical Diffuser Exit area, in. ²	0.096

Figure 1- Shrouded Impeller Volute Pump



TEST FACILITY DESCRIPTION

Testing was conducted at the Lima Test Stand of the Advanced Propulsion Test Facility (APTF) at the Santa Susana Field Laboratory of Rocketdyne. Lima Stand has liquid oxygen (LOX), liquid hydrogen (LH₂), liquid nitrogen (LN₂), gaseous hydrogen (GH₂), helium and nitrogen flow capability. Only gaseous and liquid hydrogen were used for this test series. Liquid hydrogen was used as the pumped fluid and to cool the bearings, and gaseous hydrogen was used to drive the turbine. A schematic of the test facility showing the test article is shown in Figure 2. Gaseous hydrogen for turbine drive is supplied from a 5,000 psig, 602 ft³ bottle supply. The gas flows through the run line to a servo controlled valve for control of GH₂ turbine inlet pressure independent of bottle supply pressure. The gas then passes through a 10 micron filter and precision critical flow nozzle for GH₂ flow rate measurement. Ports are also provided for pressure and temperature measurements.

Liquid hydrogen is supplied to the tester for bearing coolant and at the pump inlet from a 15,000 gallon tank rated at 100 psig. Due to the long lengths of small diameter inlet and discharge lines, it was anticipated that chilling the flow systems and providing liquid hydrogen of proper condition to the pump inlet would be difficult. Consequently, the facility lines were reworked to utilize insulated jacketed lines with hydrogen of proper condition to the pump inlet would be difficult. Consequently, the facility lines were reworked to utilize insulated jacketed lines with hydrogen flowing in the jacket as well as the line itself. During the rework, instrumentation was added to determine the quality of the hydrogen entering the pump. The pump flow supply system includes a shut-off valve, flow venturi system, a 10 micron-filter, and the pump inlet throttle valve. The pump discharge line contains a flow venturi system and the throttle valve. The bearing supply line includes an orifice and necessary instrumentation to measure bearing flow rate and temperature. Pump discharge flow and bearing overboard drainage are dumped into a burn stack. A picture of the completed test stand with the pump/turbine tester installed is presented in Figure 3.

Test data were collected on a 128 channel, computer based system capable of taking 50,000 measurements per second. The system consists of a NEFF series 620 data acquisition subsystem and a Data General Eclipse S140 computer. The computer has 256 kilobytes of memory, 256 megabytes of storage on a fixed disc, and 126 megabytes of storage on a removable disc. Associated with the computer are three video terminals. Two terminals are for displaying facility and test data for the operations personnel. The third terminal is the operator's terminal.

Data were recorded on magnetic tape during a test. Scaled data were available post-test imprinted from a 600 line-per-minute printer. The tape format is compatible with Rocketdyne's link to Rockwell's Western Computer Center, so that more extensive data reduction was provided on a 24-hour turnaround basis.

Three, six-channel Watanabe strip chart recorders were used to monitor key parameters as backup and to assist the test engineer in determining trends and/or necessary adjustments in the test plan.

Figure 2 - LH2 Test Facility Schematic

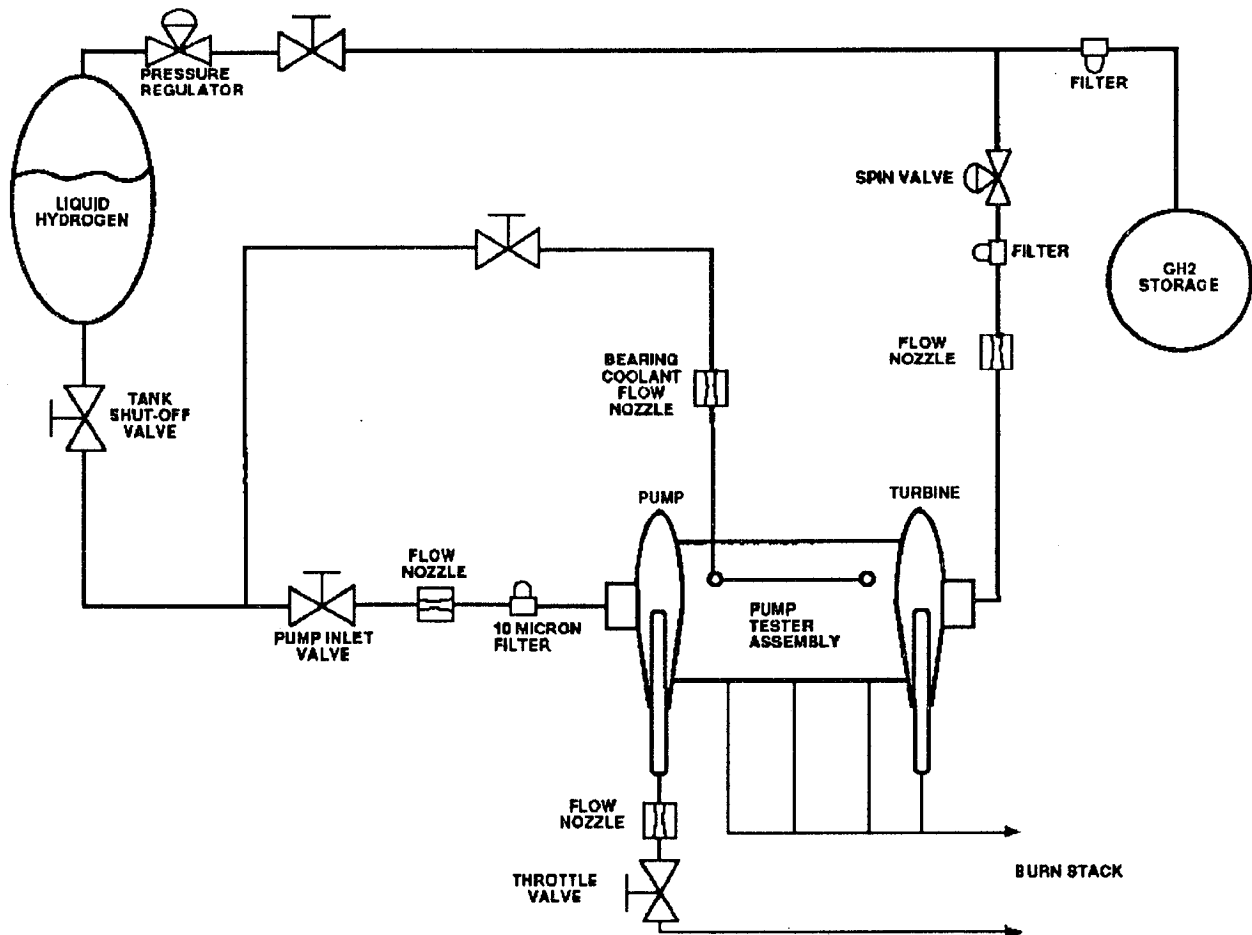
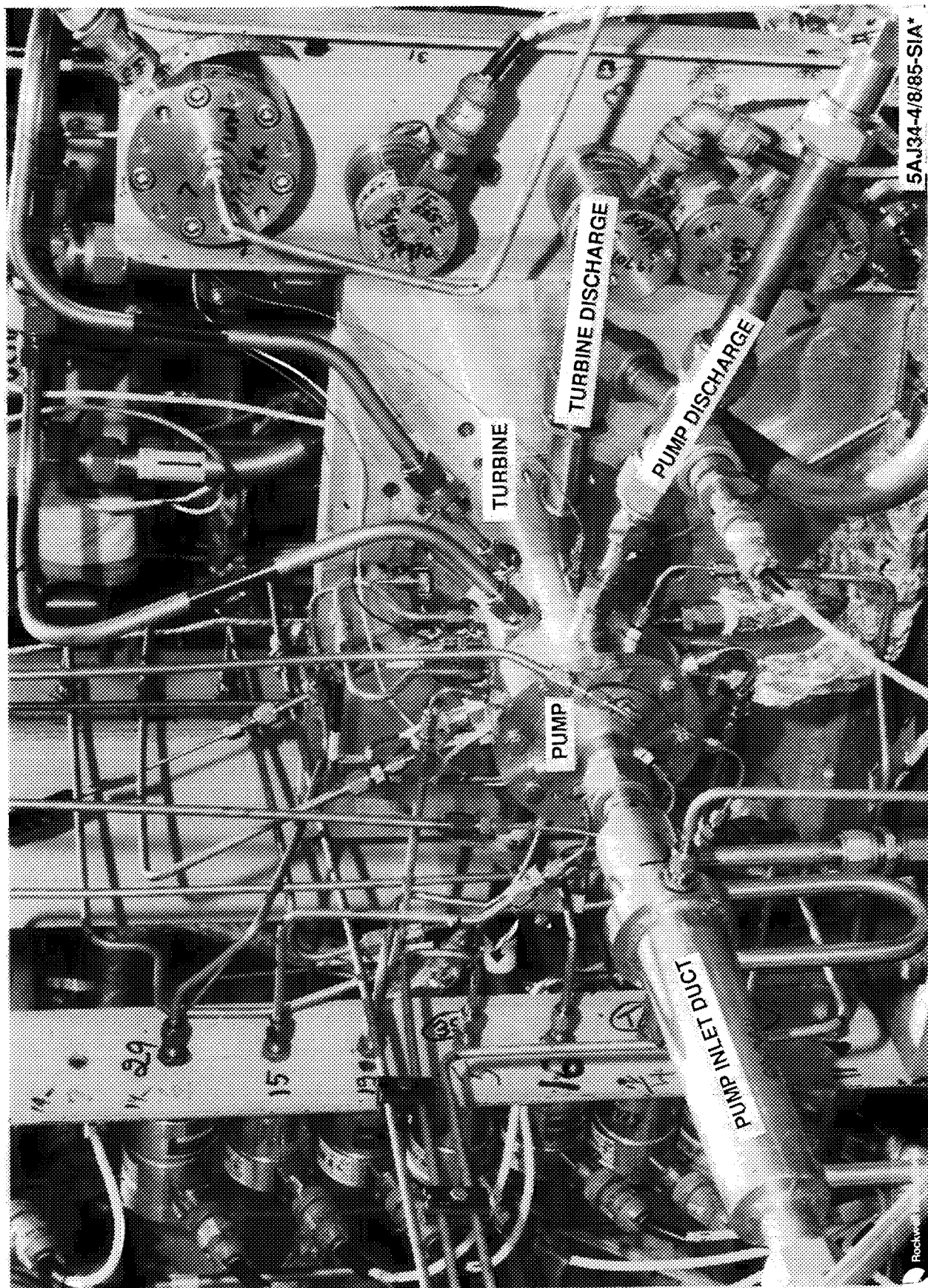


Figure 3 - Pump / Turbine Test Stand Installation



TEST PROGRAM

TEST ARTICLE

The low thrust pump/turbine tester is essentially a small turbopump with self contained turbine drive and centrifugal pumping element. For hydrogen testing, the tester turbine was driven by gaseous hydrogen supplied at ambient temperature and exhausting to a burn stack. The pumped fluid was liquid hydrogen. A cross sectional view of the pump/turbine tester and photograph of the assembled unit are shown in Figure 4 and Figure 5 respectively. The assembled unit was the same configuration as for the previously reported water testing except that the carbon face seal between the pump and tester was replaced with a labyrinth seal, and the impeller smooth surface wear ring seals were reworked to labyrinth configurations by machining labyrinth grooves in the housings. Also, the conventional oil lubricated bearings used in the water tests were replaced with bearings suitable for use in liquid hydrogen.

INSTRUMENTATION

Typical pump and tester instrumentation is shown in Figure 6 and 7. Overall (flange to flange) head rise was determined by measuring the difference in pressure between a four-hole static pressure piezometer ring located 5 diameters upstream of the pump inlet and a four-hole static pressure piezometer ring located 10 diameters downstream of the pump discharge. The velocity heads calculated from the pump flow rate and respective cross-sectional areas at the measurement stations were added to the inlet and discharge static heads to obtain the total head rise. Static pressure measurements within the pump at the tap locations noted on Figure 6 were used to calculate pump impeller radial and axial loads. Pump inlet flow rate and pump discharge flow rate were measured by means of venturi tubes. Speed was measured using eddy current proximity probes that sensed the rotation of a 0.004 inch depression machined on the tester shaft. Housing mounted accelerometers which measured pump-end radial, turbine-end radial and axial vibrations were monitored during testing to ensure safe operation.

Instrumentation is listed in Table III. Instrumentation accuracies are given in Table IV. All instrumentation was calibrated by standards traceable to the Bureau of Standards prior to testing. Calibrations were checked pretest and post-test.

TEST PROCEDURES

The tests evaluated head rise versus flow at shaft speeds of approximately 46000 and 62000 RPM. The flow rate was controlled by a throttle valve located downstream of the pump. Pump speed was controlled by varying the turbine inlet pressure to control the power input to the pump. Flow rate was varied from approximately 60 to 120% of design flow.

Suction performance tests were conducted by gradually lowering pump inlet pressure from approximately 80 psig to a low value which caused in excess of 5% pump head loss. Each cavitation test was cut automatically when pump head dropped more than 10%.

Input power to the pump was determined by computing the output power generated by the drive turbine (which had been calibrated as part of the water test series) and subtracting the tester bearing and seal drag loss. Turbine pressure and temperature measurement locations during the pump tests were the same as those for the calibration tests to provide a direct relationship of calibration information. Test drag was experimentally determined by removing the centrifugal pump and running the tester rotating assembly with liquid hydrogen as the bearing coolant and the calibrated turbine as the power source.

**Figure 4 - Pump / Tester Cross Section
(NOT TO SCALE)**

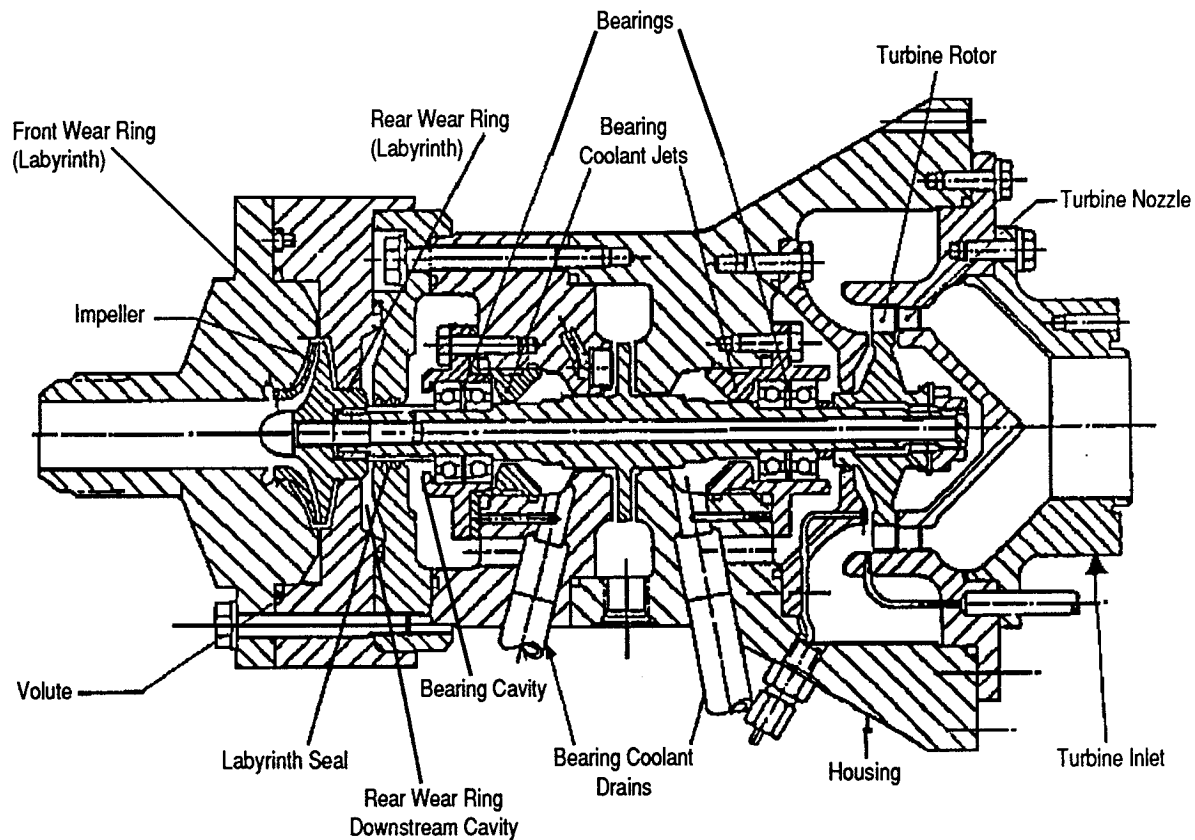
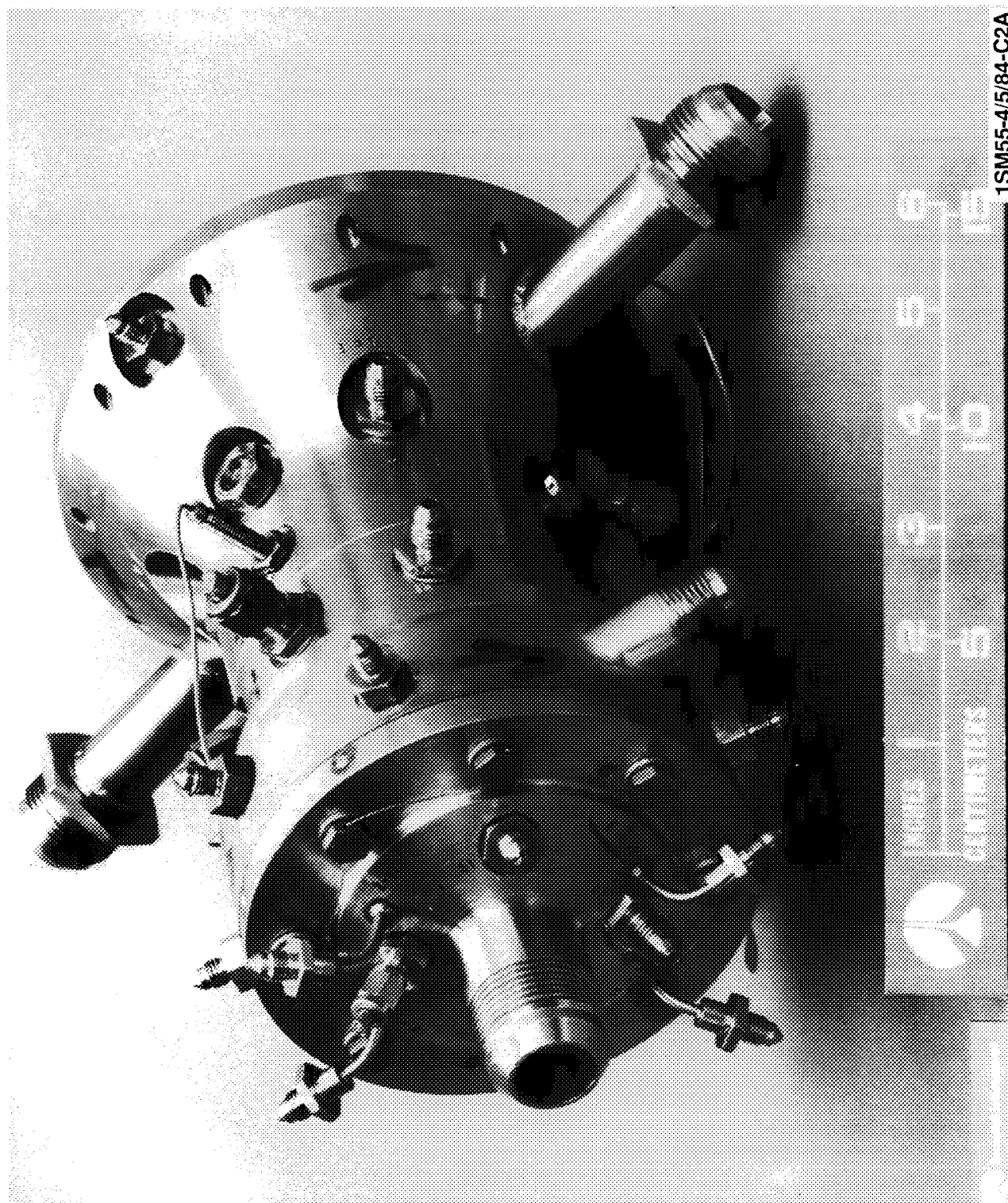


Figure 5 - Pump / Tester Assembly



ORIGINAL PAGE
BLACK AND WHITE PHOTOGRAPH

Figure 6 - Typical Pump Instrumentation

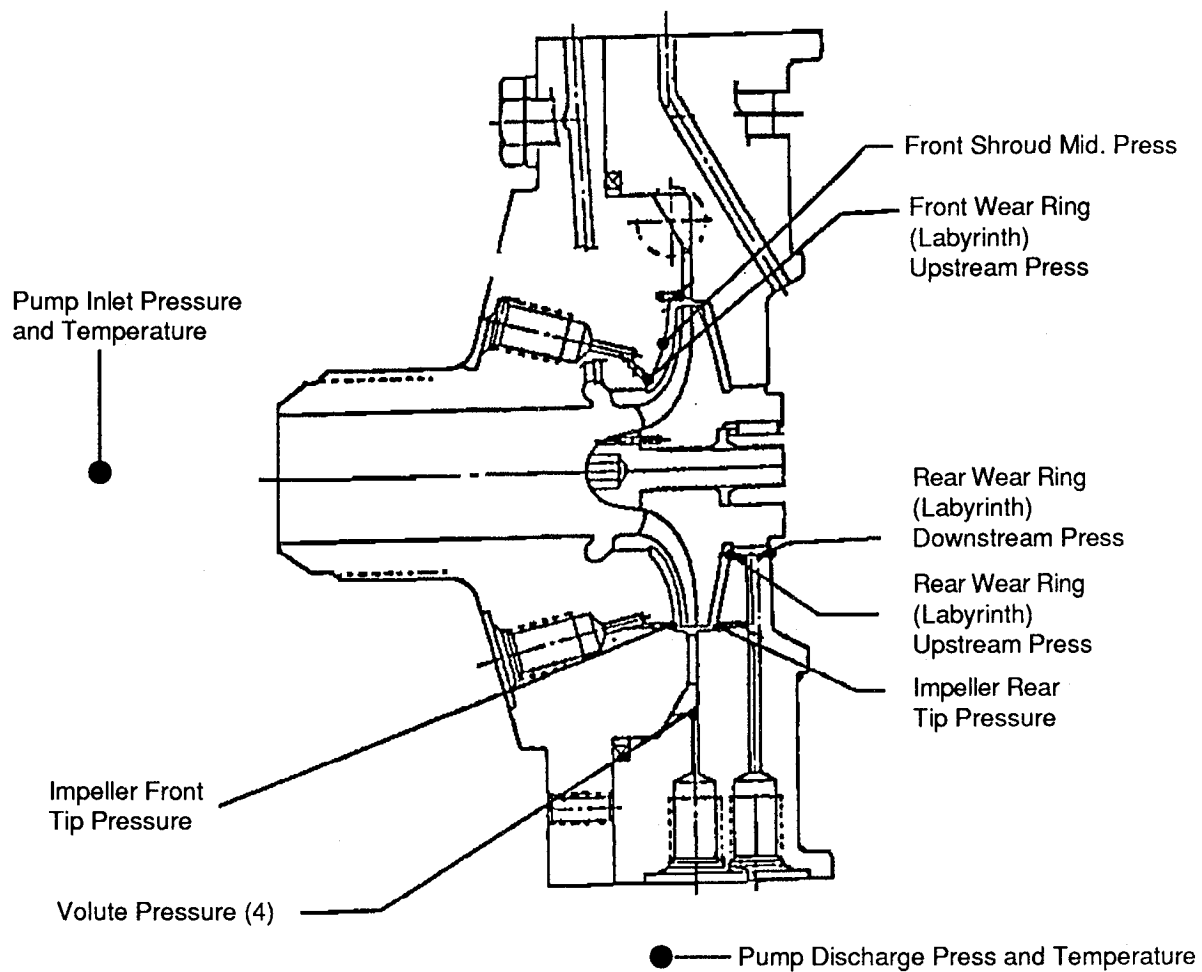


Figure 7 - Tester and Turbine Instrumentation

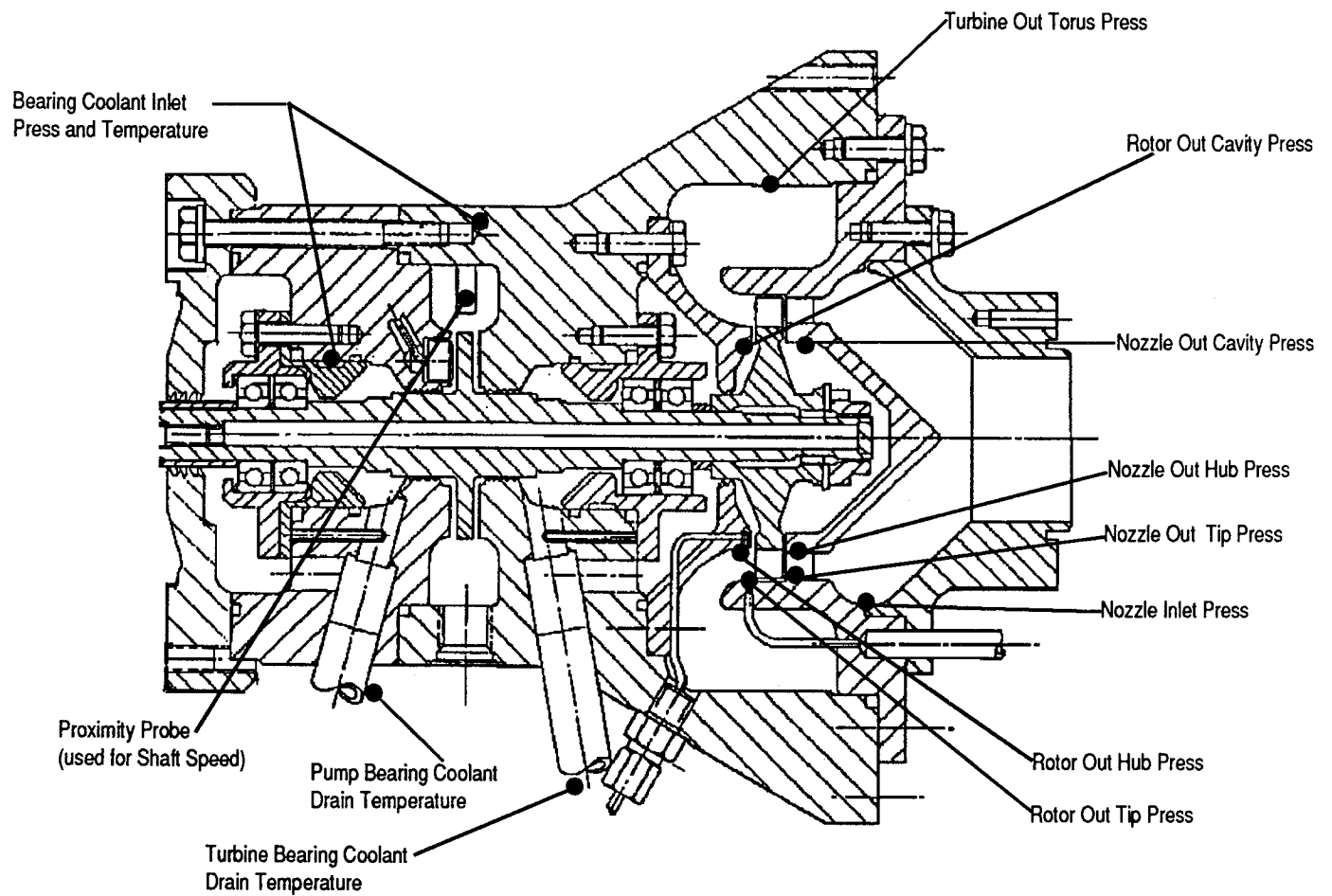


Table III - LH2 Centrifugal Pump Test Instrumentation LIST

<u>Parameter</u>	<u>Range</u>	<u>Redline</u>	<u>Low</u>	<u>High</u>
Pump Inlet Temperature	0 to 100 R	44 R		X
Pump Outer Temperature	0 to 200 R			
Bearing Coolant Inlet Temperature	0 to 100 R	47 R		X
Pump Bearing Coolant Drain Temperature	0 to 200 R	100 R		
Turbine Bearing Coolant Drain Temperature	0 to 200 R	100 R		X
Turbine Inlet Temperature	450 to 550 R			
Turbine Outlet Torus Temperature	400 to 550 R			
Pump Inlet Pressure	0 to 100 psig	60 psia	X (H-Q Tests only)	
Pump Discharge Pressure	0 to 500 psig			
Volute Discharge Pressure - 0 Degrees	0 to 500 psig			
Volute Discharge Pressure - 90 Degrees	0 to 500 psig			
Volute Discharge Pressure - 180 Degrees	0 to 500 psig			
Volute Discharge Pressure - 270 Degrees	0 to 500 psig			
Front Wear Ring Upstream Pressure	0 to 500 psig			
Rear Wear Ring Upstream Pressure	0 to 500 psig			
Rear Wear Ring Downstream Pressure	0 to 250 psig			
Impeller Front Tip Pressure	0 to 500 psig			
Impeller Front Mid Pressure	0 to 500 psig			
Impeller Rear Tip Pressure	0 to 500 psig			
Turbine Nozzle In Pressure	0 to 50 psia	25 psia		
Turbine Nozzle Out Tip Pressure	0 to 100 psig			
Turbine Nozzle Out Hub Pressure	0 to 100 psig			
Rotor Out Tip Pressure	0 to 100 psig			
Rotor Out Hub Pressure	0 to 100 psig			
Turbine Nozzle Out Cavity Pressure	0 to 100 psig			
Rotor Out Cavity Pressure	0 to 100 psig			
Turbine Out Torus Pressure	0 to 50 psia			
Bearing Coolant Inlet Pressure	0 to 100 psig	60 psig	X	X
Bearing Coolant Inlet Orifice Pressure	0 to 100 psig			
Pump Inlet Valve Inlet Temperature	0 to 100 R			
Pump Inlet Venturi Temperature	0 to 100 R			
Pump Inlet Venturi Pressure	0 to 100 psig			
Pump Inlet Valve Inlet Pressure	0 to 100 psig			
Shaft Speed, Rpm (2 Bently's)	0 to 85,000	Varies per test	X	
Bearing Coolant Inlet Orifice Delta-p	0 to 20 psid			
Pump Radial Acceleration, Vibration	0 to 50 G, Rms	20 G Rms		X
Turbine Radial Acceleration, Vibration	0 to 50 G, Rms	20 G Rms		X
Axial Acceleration, Vibration	0 to 50 G, Rms			
Time-irig, Seconds				
Pump Discharge Flow Venturi Delta-p	0 to 20 psid			
Pump Inlet-discharge Depta-p	0 to 250 psid			
Pump Inlet Flow Ventura Delta-p	0 to 20 psid			
Turbine Flow Nozzle in Temperature	450 to 550 R			
Turbine Flow Nozzle in Pressure	0 to 1000 psig			
Turbine Flow Nozzle Out Pressure	0 to 100 psig			
Bently (3) Vibration	0 to .015 inch, P-P	.010 inch, P-P		X

*Barometric Pressure Recorded for Test Period

Table IV - Instrumentation Accuracies

Pump Inlet Pressure	±0.5 PSI
Pump Inlet and Discharge Temperature	±0.2 Degree R
Pump Discharge Pressure and ALL OTHER	±2.5 PSI
Internal Pressures Shown in FIG. 6	
Flow Rate	±0.5%
Shaft Speed	±0.5%

TEST MATRIX

Liquid hydrogen tests were performed at two speeds and four flow rates per speed at non-cavitating conditions. Cavitation data were obtained at three flows for one speed. The tests are listed in Table V.

Table V - Test Matrix

<u>Test Number</u>	<u>Testing Details</u>
016024	H-Q testing at 60% Design speed (46200 RPM) Flow range .7 to 1.6 Q/QD
016026	H-Q testing at 80% Design speed (61600 RPM) Flow range .7 to 1.4 Q/QD Cavitation test at 80% Design speed (61600 RPM) Flow of .65 Q/QD
016027	H-Q testing at 80% Design speed (61600 RPM) At design flow Cavitation test at 80% Design speed (61600 RPM)

TEST RESULTS

Liquid hydrogen testing of Test Configuration #2 consisted of non-cavitating and cavitating performance tests over a range of rotational speeds and hydrogen flow rates. The pump design speed and flow rate are 77,000 RPM and 15.7 GPM, respectively. A rotordynamic vibration was encountered during testing between 70,000 and 75,000 RPM. The planned test speed of 77,000 RPM was reduced to avoid potential component damage. Review of the test data confirmed the presence of a critical speed at about 74,000 RPM. The predicted value of the first critical was 96,000 RPM. The difference was probably due to the larger than desired dead band found in one bearing assembly. Successful non-cavitating tests were run at 60 percent design speed, and a series of cavitating and non-cavitating tests were conducted at 80 percent design speed.

HEAD-FLOW

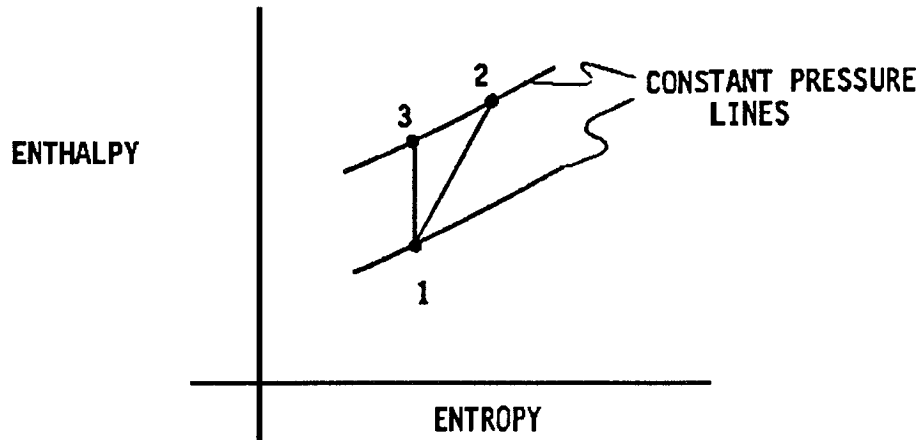
The head produced by the pump is determined from measurements between a point upstream of the pump inlet and a point downstream of the volute discharge. The thermodynamic states upstream and downstream of the pump are known from measured pressures and temperatures. The discharge state reflects an increase in energy over the inlet state due to pumping of the fluid and also due to pump losses resulting in internal fluid heating. The isentropic process line 1-3 of Figure 8 is used to determine the ideal pump head. The process 1-2 is the actual process including losses.

The isentropic head for the two test speeds in hydrogen is plotted in Figure 9 with all data scaled to a speed of 77,000 RPM. Two data sets were derived from test 016-024 (test shaft speed of 46200 RPM). The first set, represented by solid squares in Figure 9, was obtained while operating at a fixed steady state flow. The second set, represented by circles, was obtained while the flow rate was in a slow transient from 1.3 to 0.7 times design flow. It is observed that both sets align well with each other. This agreement is not always true for transient data because of lag in sensing ports and/or data acquisition equipment.

The measured head in hydrogen is relatively flat over the test flow range similar to the head/flow characteristic from the water test results given in reference 1 and shown here in Figure 10. As discussed in reference 1, leakage flow which is recirculated through the impeller strongly influenced the shape of the curve. The leakage includes rear wear ring flow which is returned to the inlet through passages in the test article and front wear ring flow which mixes with the inlet flow after passing through the wear ring. The front wear ring flow has a large tangential velocity component prior to mixing with the incoming flow. This produces prewhirl at the impeller inlet which drops the change of angular momentum produced by the impeller and therefore reduces pump head rise. As the delivered pump flow is reduced, the ratio of impeller total flow to whirling front wear ring flow is decreased. This acts to reduce pump head rise at reduced delivered flow while the increased tangential velocity at the impeller blade exit acts to increase the pump head rise. The result is a nearly constant head rise as delivered flow is reduced.

The scaled head rise data in Figure 9 also indicate that the isentropic head coefficient of the pump decreased as test speed was increased. This is typical of hydrogen pump operation in that at higher speeds (pressures) the head rise does not follow similarity relations because of hydrogen compressibility and thermodynamic property effects.

Figure 8 - Isentropic Head Flow



Where:

- 1 - Inlet State
- 2 - Actual Discharge State
- 3 - Ideal Discharge State

The calculated pump head is:

$$\Delta H = (h_3 - h_1) 788.2$$

Where:

- ΔH - Head (feet)
- h - Enthalpy (btu/lbm)

Figure 9 - Low Thrust Hydrogen Test, Configuration 2
Head-Flow Testing

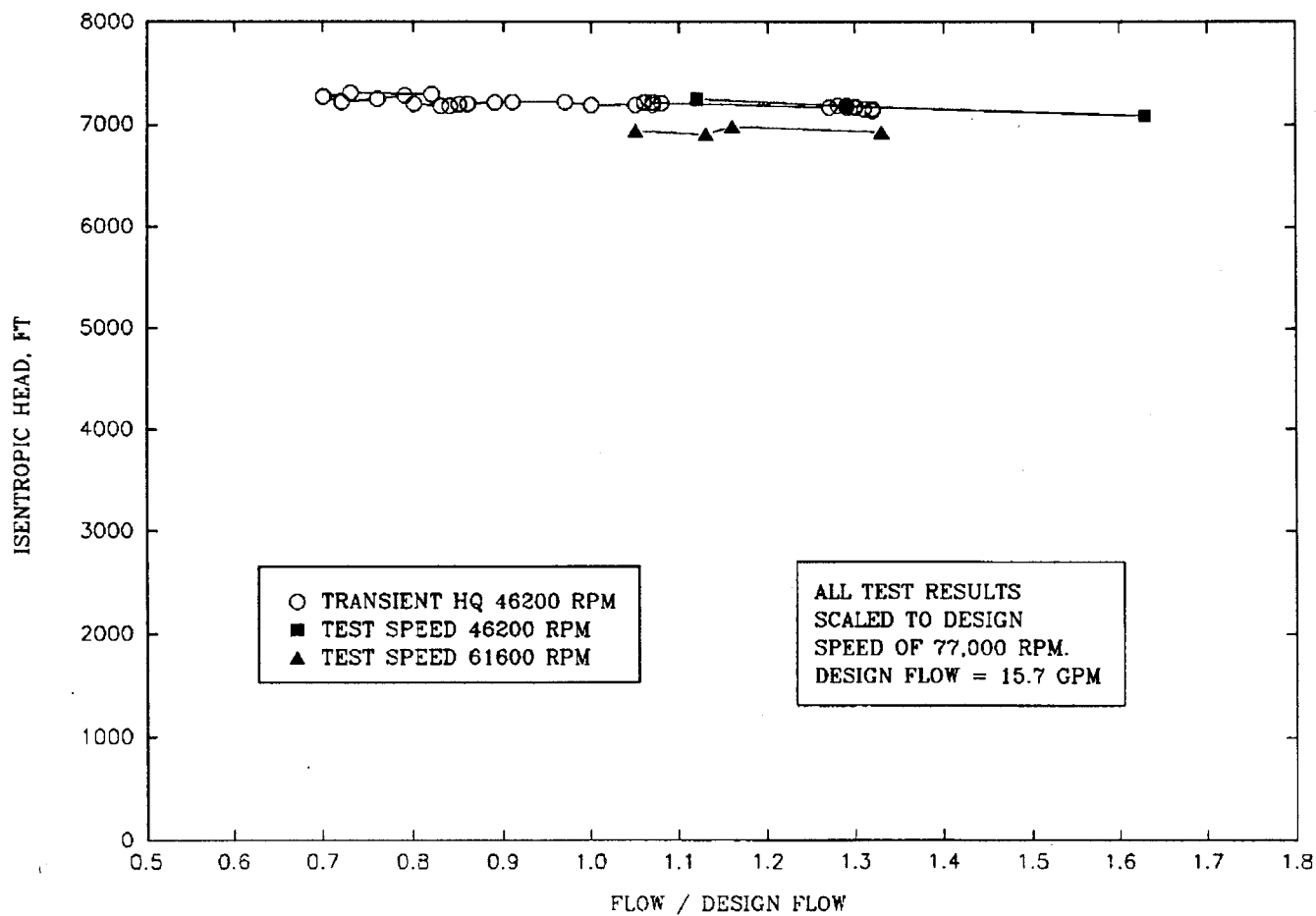
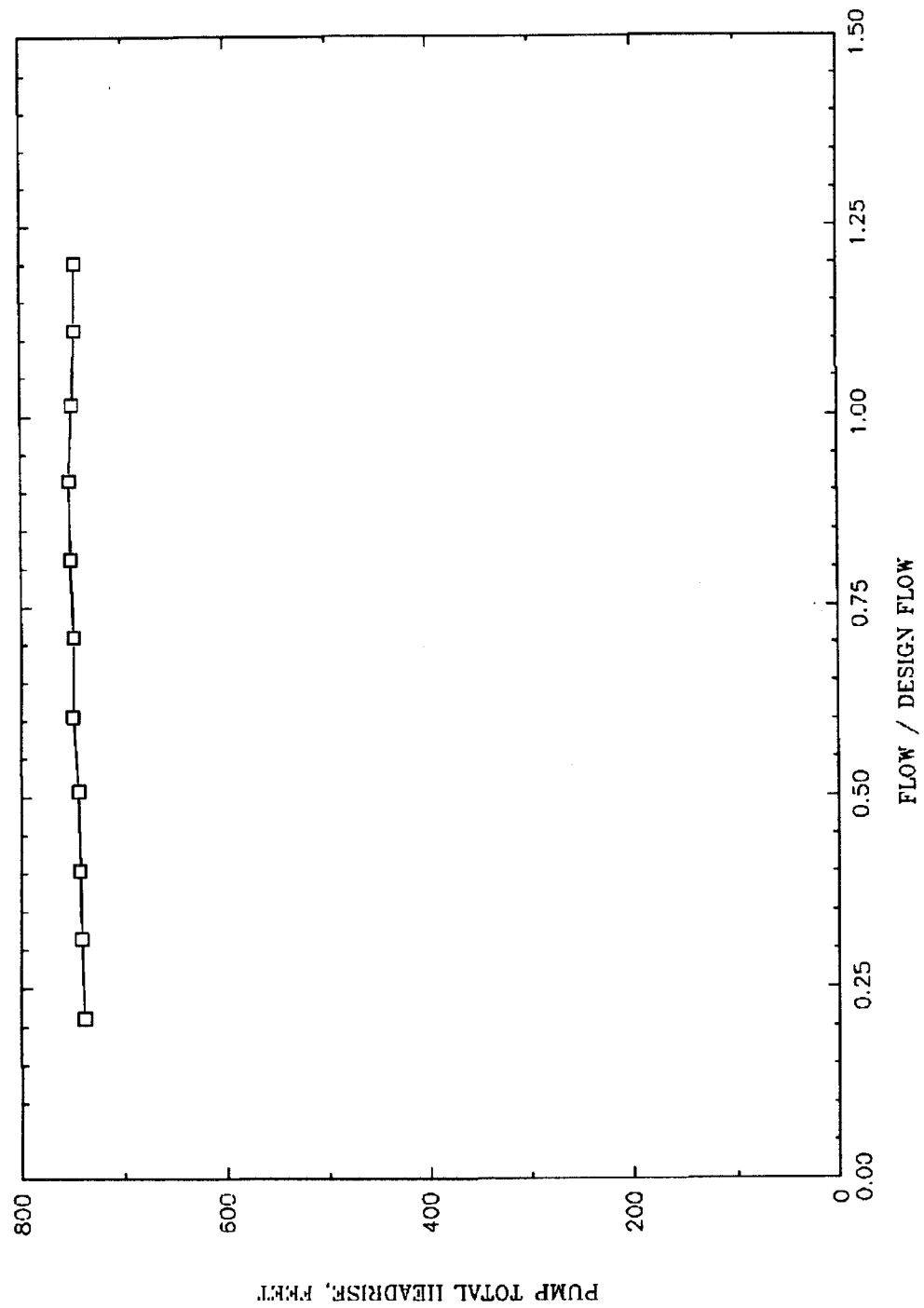


Figure 10 - LOW-Thrust Water Testing
Configuration 2,
Test and Curve Speed - 24,500 RPM



PUMP EFFICIENCY

Enthalpy Basis The pump isentropic efficiency can be determined from the ratio of enthalpy gain in the ideal process to the actual process when no overboard flow losses exist.

$$\eta = \frac{h_3 - h_1}{h_2 - h_1}$$

In the configuration which was tested, an efficiency correction is required to account for the heated fluid being lost through the shaft labyrinth seal into the bearing cavity (See Figure 4). This amount of overboard flow is the difference between the pump inlet and discharge flows which were measured during the tests. The overboard flow is primarily a function of the pressure difference between the rear wear ring downstream cavity and the bearing cavity. Wear ring pressure is measured during testing.

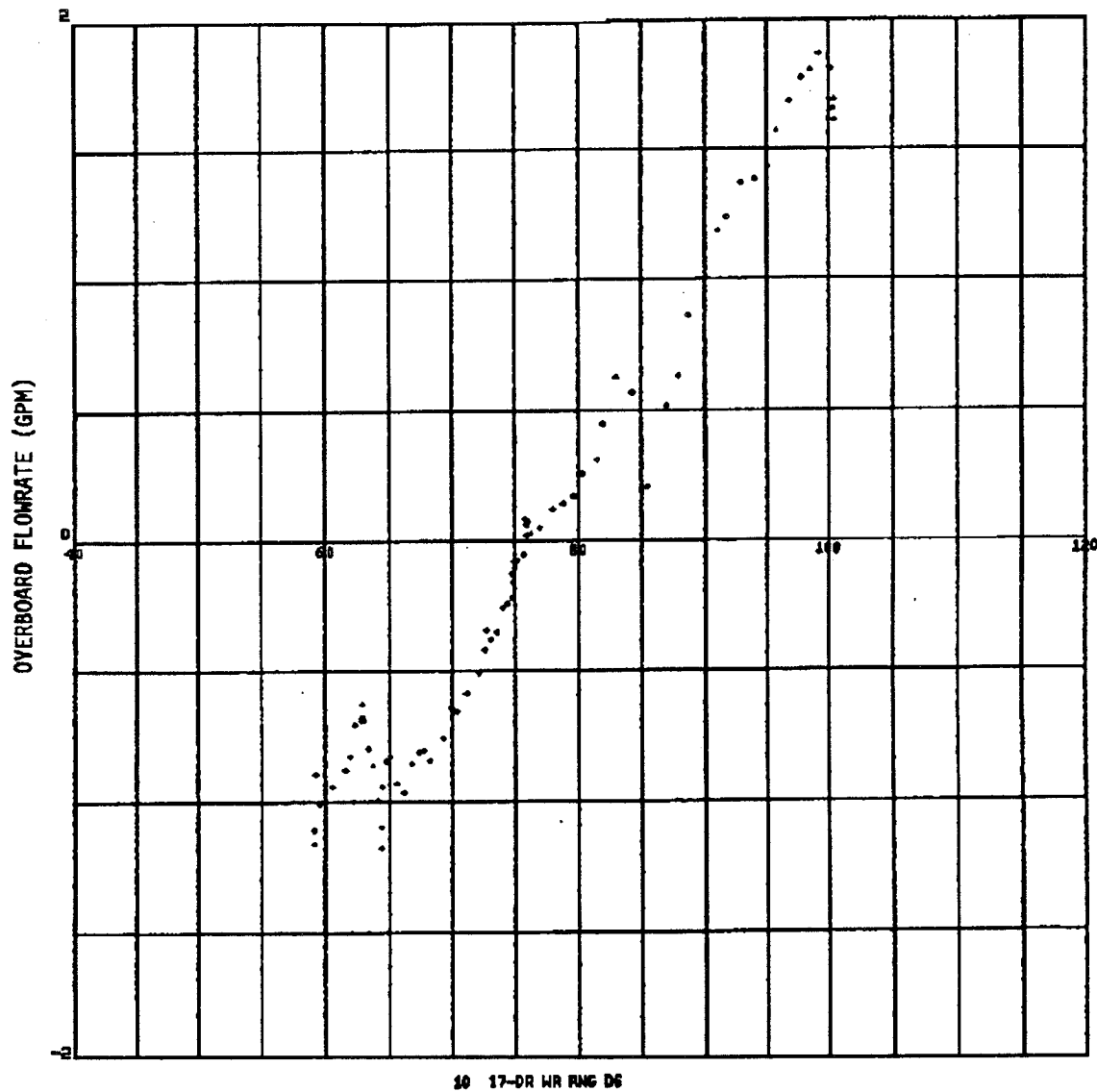
The bearing cavity pressure was nearly constant throughout the test. The bearing cavity pressure can be determined from cavitation test data. During cavitation testing, pump pressure is decreased to the point where there is no overboard flow, as shown in Figure 11. The bearing cavity pressure is 76 psig compared to a bearing supply pressure of 80 psig. At a flow rate of 93% of design, the pump efficiency with no overboard flow is two percentage points lower than the uncorrected efficiency measured during the flow tests. This correction for overboard flow is applied to the entire flow range tested since the overboard flow rate did not vary significantly during H-Q testing.

The corrected values for pump isentropic efficiency are plotted in Figure 12 along with the water test efficiencies. This figure also includes the corrected efficiency of the pump during the transient portion of test 016-024. The efficiency plot for the transient test exhibits more scatter than corresponding head data in the previous discussion. The data scatter is caused by transducer accuracy during the transients and not oscillations from the pump.

Referring to the previous section (HQ discussion), the head of the pump was almost flat. From the efficiency plots it is seen that the efficiency is increasing with flow even above the design flow. The efficiency increases with flow because the ratio of recirculation to incoming flow decreases. Since impeller head remains fairly constant, the recirculated flow also is constant. However, as the incoming flow increases while the recirculating flow remains constant, the impact on efficiency is less. It is not unusual for a low specific speed pump to have its efficiency strongly driven by the seal leakage rates.

Turbine Power Basis Pump efficiencies based on turbine output power have been corrected to include the losses from the tester drag torque for pump Configuration #2. To make this correction the tester is considered as three components: the turbine, the tester and the pump. Turbine calibration was completed as part of the water testing series, and the resulting turbine performance characteristic is presented in Figure 13. For liquid hydrogen testing, liquid hydrogen was used to lubricate the bearings. A tester drag calibration test was conducted with liquid hydrogen supplied to the bearing lube jets, and the resulting tester drag torque characteristic is plotted in Figure 14.

Figure 11 - Low Thrust Hydrogen Testing, Configuration 2
Test 016027, Shaft Speed 61,600 RPM



ADVANCED PROPULSION TEST FACILITY Test 016027

Frame 59

Rear Wear Ring Downstream Cavity Pressure (Psig)

Figure 12 - Low Thrust Hydrogen Test, Configuration 2
Isentropic Pump Efficiency

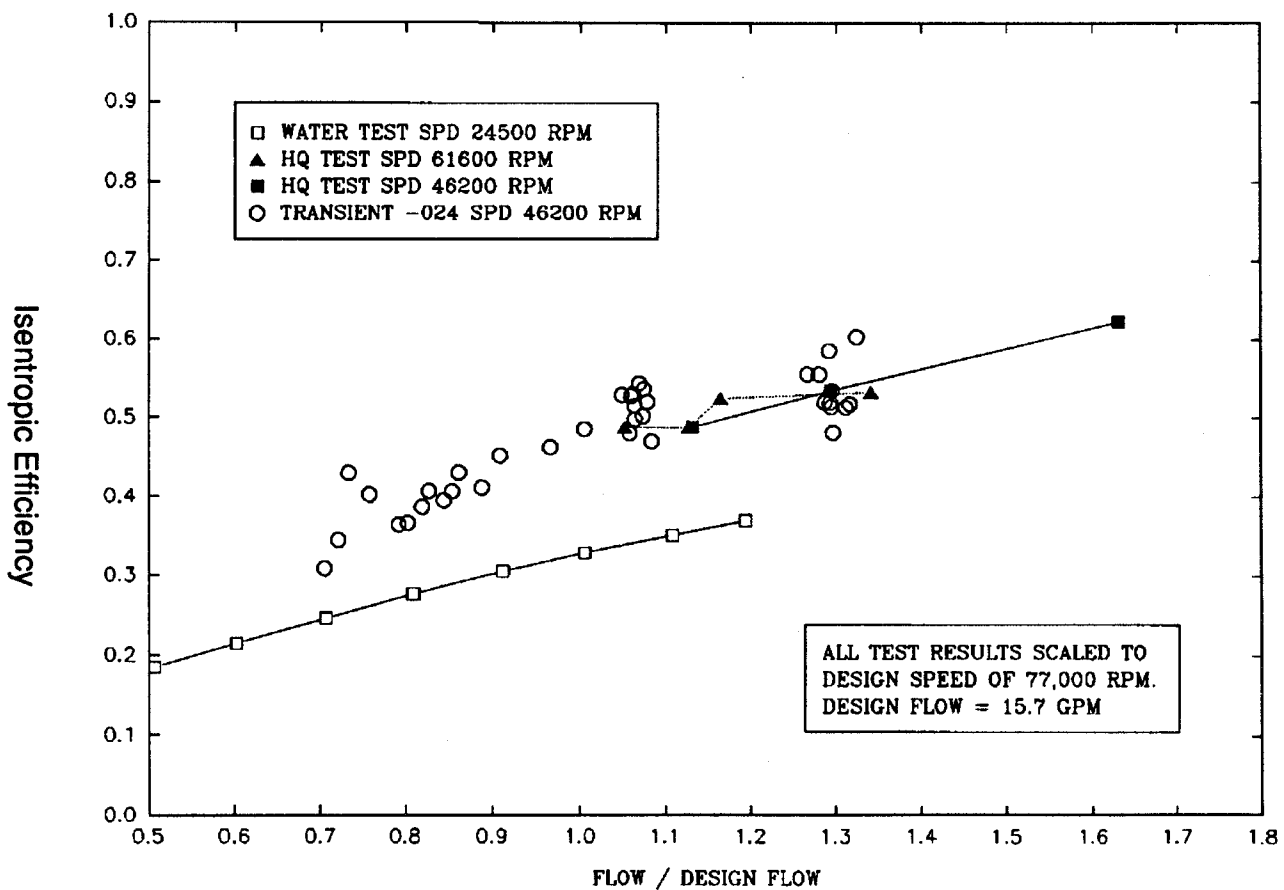
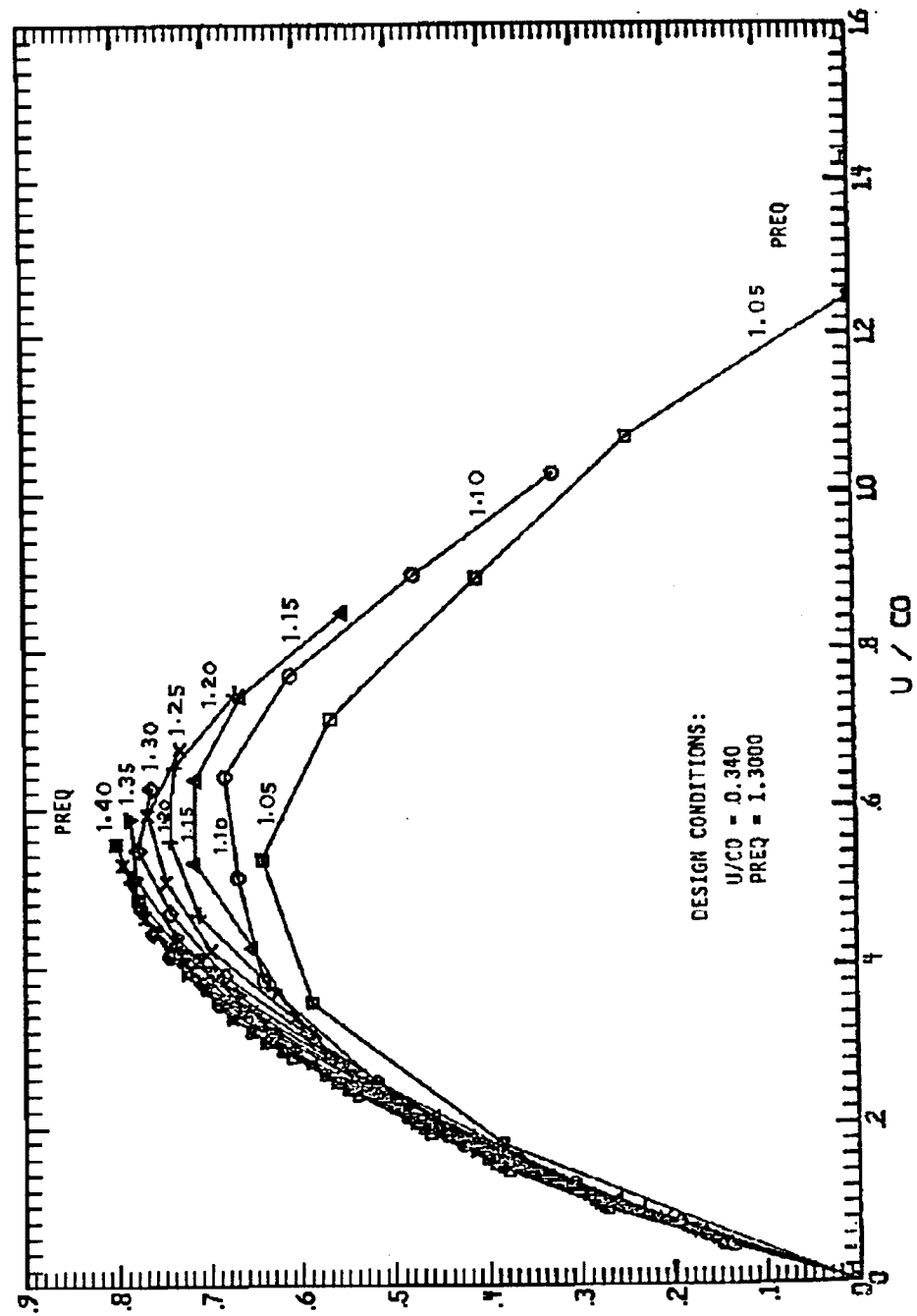
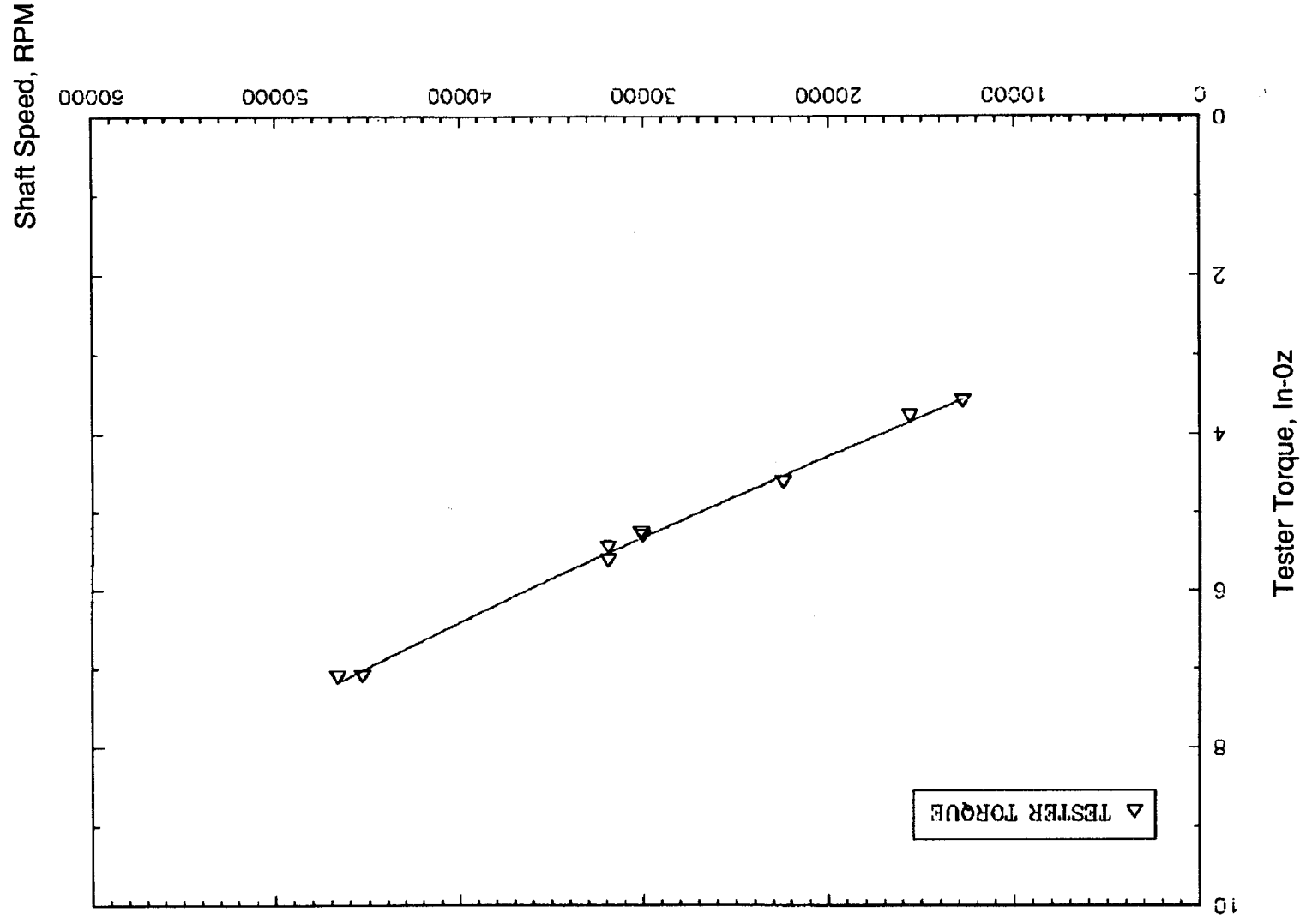


Figure 13 - Low Thrust Turbine Efficiency
100 Percent Admission



EFF Final Curve

Figure 14 - Low Thrust Tester Torque
Liquid Hydrogen Lubrication



To correct the pump efficiency for tester drag, a linear curve fit to the tester drag torque was extrapolated to cover the full range of shaft speeds tested. By subtracting the bearing drag from the turbine output power, the pump input power was found. The pump hydraulic output power was then divided by this input power to determine the pump efficiency.

Efficiencies for Configuration 2 in hydrogen and water based on turbine power output and bearing and seal drag calibration tests are shown in Figure 15. Also shown are the isentropic efficiencies from the steady state head-flow tests in hydrogen. The water and hydrogen efficiencies based on turbine power which are based on ideal-to-actual enthalpy increases, are shown to be 10 to 13 percentage points above the efficiencies based on turbine power. Since the hydrogen temperature rise across the pump was only about 3 degrees Rankine, the isentropic efficiencies have a high uncertainty. For example, a temperature measurement error of 0.5 degrees would cause the efficiency to vary by approximately seven points. For the turbine power based efficiencies, the temperature differential across the turbine was about 70 degrees so that a 0.5 degree error would cause an efficiency variation of only one-half percentage point in derived pump efficiency.

ANALYSIS OF PUMP LOSSES

The work conducted during the water test program included analysis of pump losses in water for Configuration #2 using the as-tested wear ring radial clearances. Results of that analysis along with results of similar analysis for the as-tested wear ring radial clearances in hydrogen are given in Table VI. Note that the losses are given as a percentage of input power for the respective pumped fluid and are not directly comparable in terms of absolute power consumption.

Comparison of the water and hydrogen losses shows that friction related loss factors in hydrogen are lower than those in water. This is due to the much lower viscosity of hydrogen and higher Reynolds numbers which reduce the friction factor to the extent that the loss factors are lower even though the hydrogen velocities are significantly higher. The largest loss factor in either fluid is wear ring leakage which is seen to be inordinately high in hydrogen because of the large as-tested wear ring clearance. As was the case in the water test program, analysis was conducted to provide an expected efficiency to reflect pump operation at the 0.002 inch design value of radial clearance. Results are given in Table VII along with the previous results for the water pump. The adjusted design point water test efficiency is 33.5 percent, and the adjusted hydrogen test efficiency is 43.7 percent.

SUCTION PERFORMANCE

Two successful cavitation tests were performed at 61,600 RPM. The target flow rates for both tests were near design, however, as the inlet pressure is steadily reduced, the flow rate also decreases. The test flow rates are representative of the flow conditions at the point of severe cavitation. Plots of pump inlet flow rate, shaft speed, isentropic head and overboard flow rate (to bearing cavity) are shown vs. pump inlet NPSH in Figure 16. The overboard flow rate is the difference between pump inlet and discharge flow rates. At high inlet pressures the net overboard flow is from the impeller rear wear ring downstream cavity past a shaft labyrinth seal to the bearing cavity. As pump pressures are lowered during cavitation testing, the flow reverses, now flowing from the bearing cavity at approximately 76 psig and below to mix with the pump wear ring flow.

Figure 15 - Low Thrust Hydrogen Test
Configuration 2

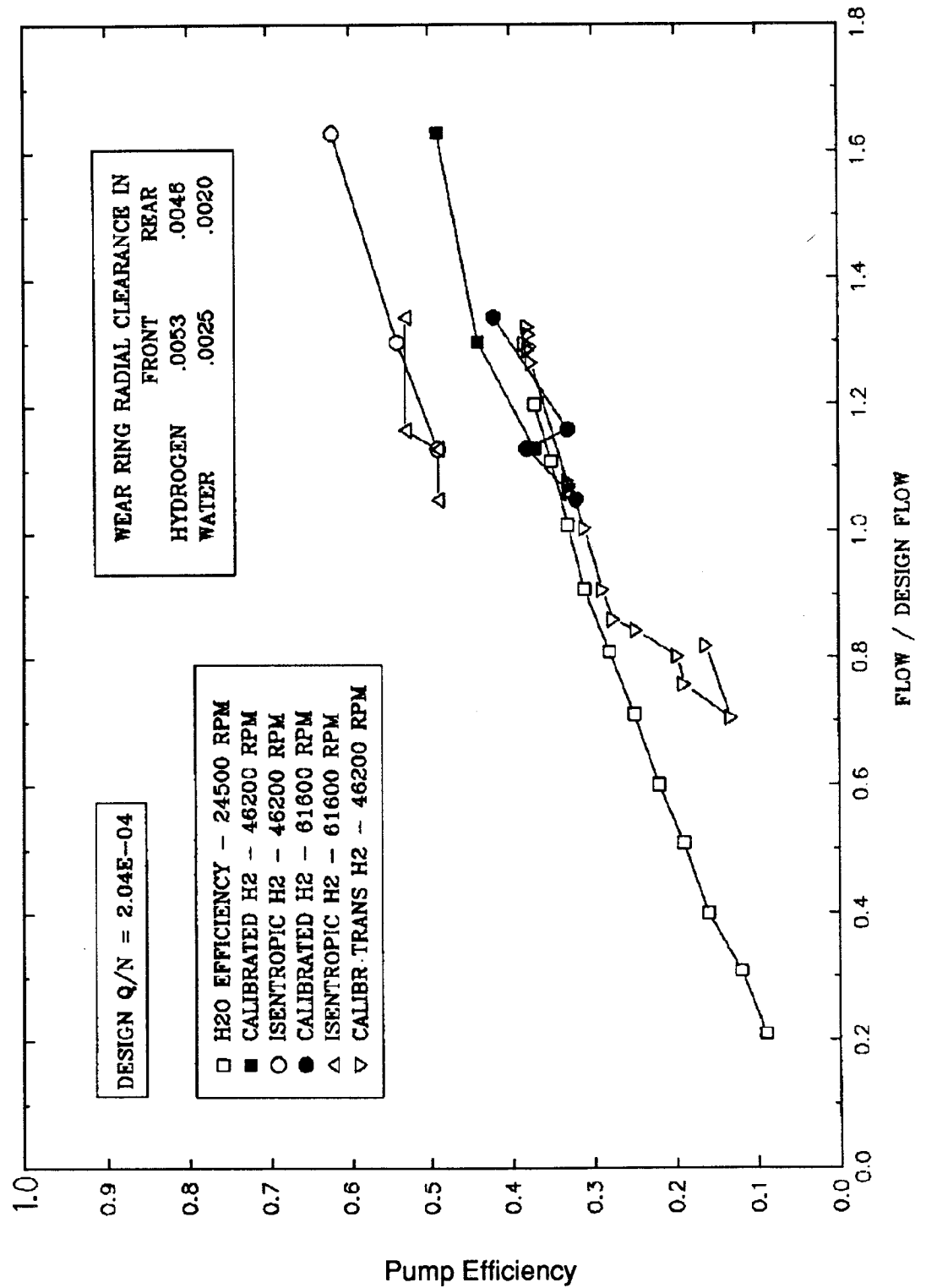
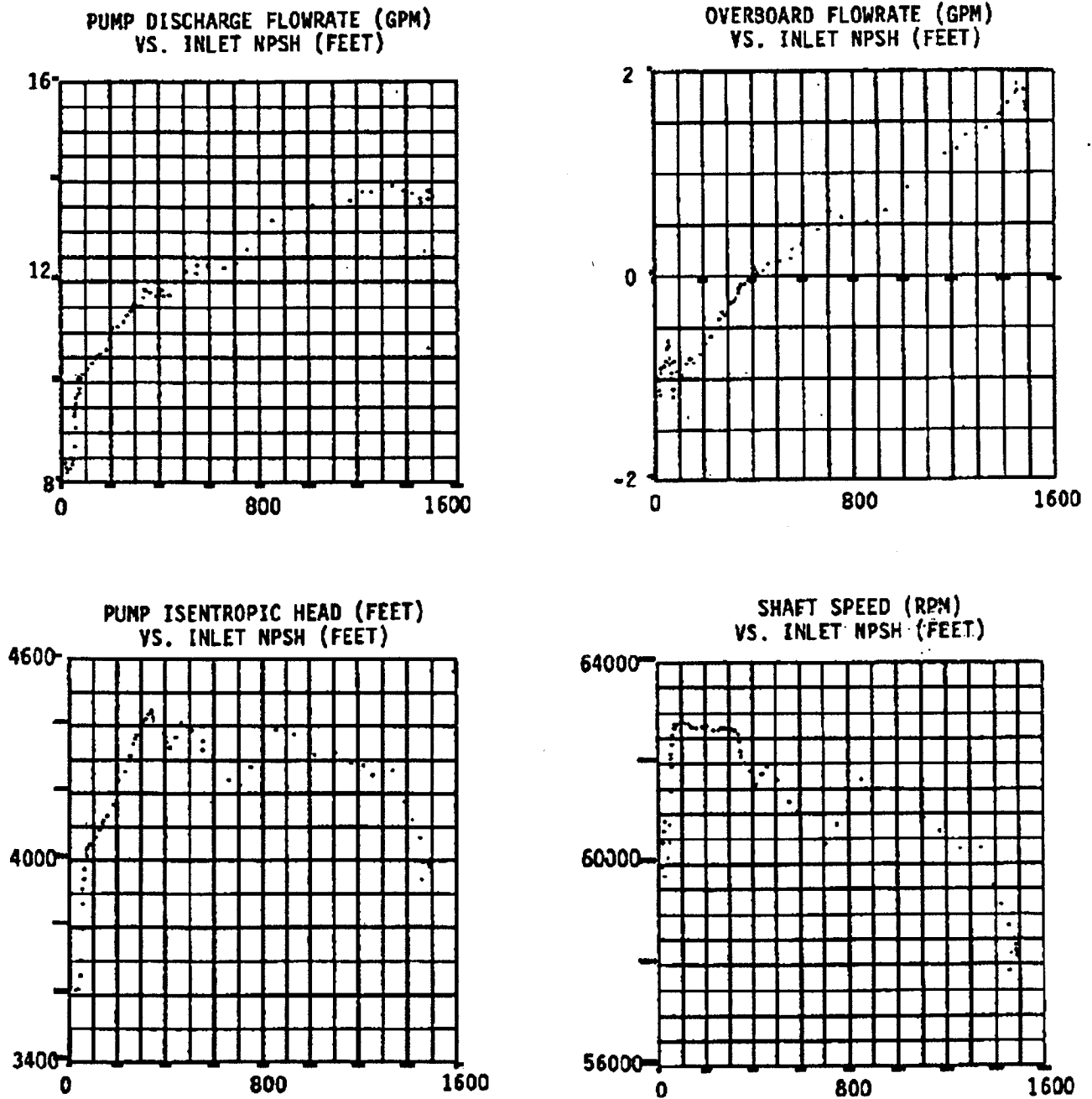


Figure 16 - Low Thrust Hydrogen Testing
Configuration 2
Cavitation Test 016027



**Table VI - Predicted Design Point Losses AS Percent of Input Power at
Operating Wear Ring Clearances
Configuration 2**

<u>Parameter</u>	<u>Water</u>	<u>Liquid Hydrogen</u>
Speed, RPM	24,500	77,000
Flow Rate, GPM	5.0	15.7
Wear Ring Radial Clearance, in		
Front	.0025	.0053
Rear	.0020	.00465
Losses as Percent of Input Power		
Total Wear Ring Leakage	28.9	51.74
Disk Friction	22.07	9.84
Impeller Internal Friction	4.65	2.73
Impeller Diffusion	.71	.44
Impeller Incidence	.62	.34
Impeller Exit Recirculation	0	0
Vaneless Space Friction	.77	.47
Volute Momentum	1.28	1.00
Volute Friction	3.78	2.37
Volute Diffusion	.22	.21
TOTAL	62.99	69.14
Predicted Efficiency, Percent	37.01	30.86

**Table VII - Design Point Pump Efficiencies
Configuration 2**

<u>Parameter</u>	<u>Water Test</u>	<u>Hydrogen Test</u>
Speed, RPM	24,500	77,000
Flow Rate, GPM	5.0	15.7
Average Wear Ring Clearance in	.00225	.00498
Test Efficiency Percent	32.5	30.3
Predicted Efficiency at Test Clearance Percent	37.01	30.86
Test Efficiency Adjusted TO .002" Radial Wear Ring Clearance	33.5	43.7

This flow is then routed to the impeller inlet. The pump isentropic head varies during the test due to shaft speed variations and due to changes in the overboard flow rate. For positive overboard flows the head follows the shaft speed squared. As the overboard flow reverses, the head is shown to decrease due to the mixing of the two flows.

Figure 17 is a re-plot of Figure 16, where the abscissa is pump flow over design flow. The left ordinate (Y-axis) is the head of the pump, and the right ordinate is the overboard flow. Results from three tests are plotted. The head from test 024 remains constant for all flows, and the overboard flow is always positive. Tests 026 and 027 have nearly constant head until the overboard flow becomes negative, that is, bearing cavity fluid mixes with the pump fluid. The pump efficiency characteristic also dropped off sharply at the corresponding pump flow at which the overboard flow became negative.

Pump cavitating performance can be characterized by the Suction Specific Speeds (Nss) parameter which is defined by the following expression:

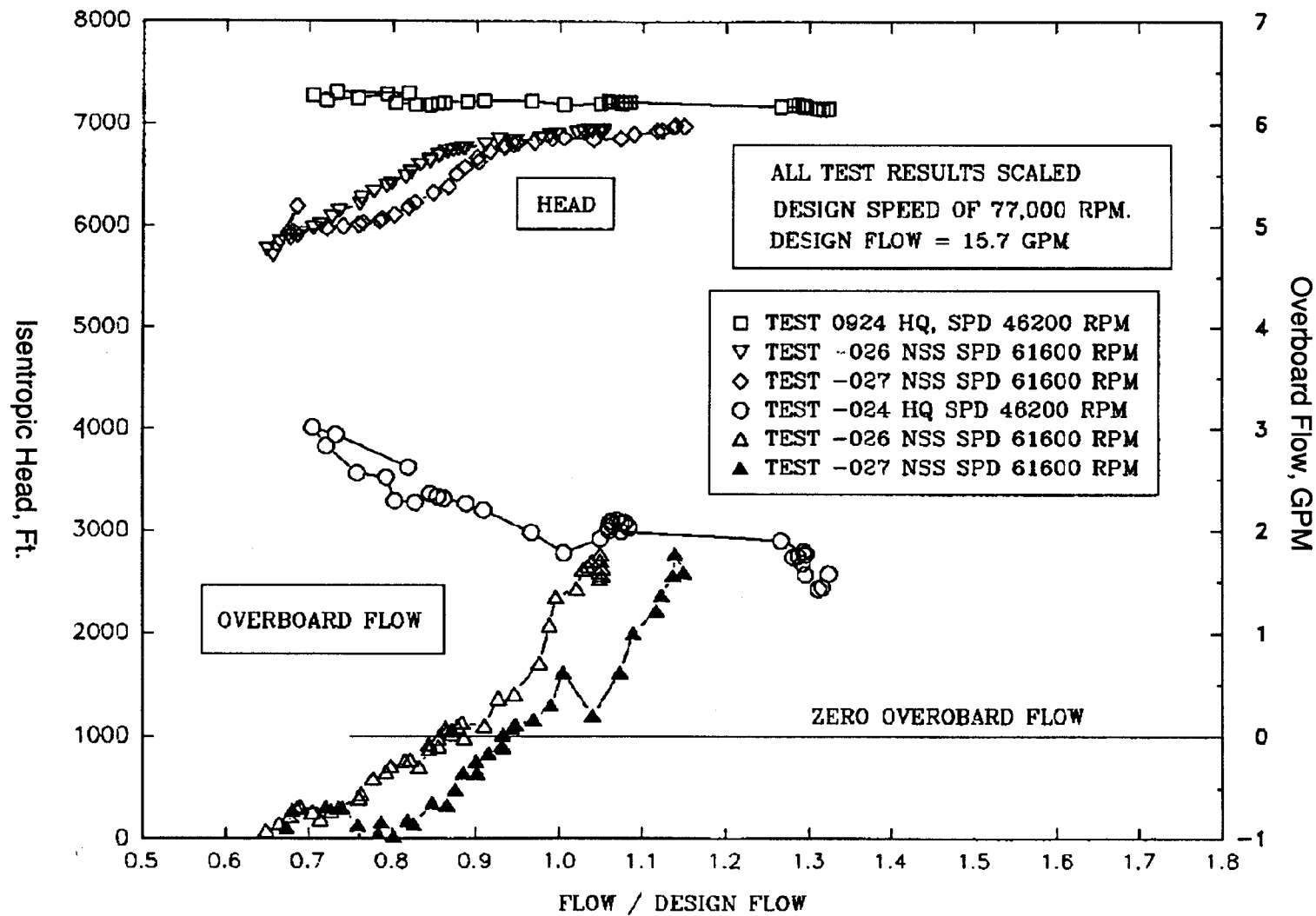
$$N_{ss} = \frac{N (Q)^{1/2}}{(NPSH)^{3/4}}$$

Where N - Shaft Speed (RPM)
 Q - Pump Inlet Flow (GPM)
 NPSH - Net Positive Suction Head at each data point (FEET)

For the hydrogen testing reported here, the cavitation performance capability of the pump is defined as the Suction Specific Speed at which the head rise of the pump is 3% less than the non-cavitating head rise.

Figures 18 and 19 are plots showing the increase in Nss as inlet NPSH was lowered during the tests. Figure 20 presents Nss as flow varied during the tests. Since inlet flow rate was

Figure 17 - Low Thrust Hydrogen Test
Configuration 2
Head-Flow Testing



decreasing as NPSH was lowered, the Nss points reflect flow rates below the design point values for the test speeds. In test 016026, the 3% head loss point occurred at an Nss of 9620 with the flow at 65% of design. In test 016027, the 3% head loss point was at an Nss of 8800 with the flow at 72% of design.

In Figure 21, the two Nss points which were obtained in the hydrogen tests are overlaid on a plot of Suction Specific Speed versus Flow Ratio from the water tests results given in Reference 1. Note that the water test results were reported at 5% head loss conditions rather than the 3% conditions for the hydrogen tests. Examination of the water head loss versus NPSH curves showed relatively steep head drop-off such that the difference in water Nss between 3% and 5% is small. As shown in the figure, both of the hydrogen Nss points reflect better suction performance than water Nss at corresponding flow ratio conditions. This is expected because of thermodynamic suppression head affects in hydrogen. With only two Nss points, an extrapolation of data to design flow conditions was not possible, especially since the two points by themselves indicate an erroneous Suction Specific Speed trend as flow ratio is increased from 0.65 to 0.72 Q/Qd. The reason for the difference in calculated Nss magnitudes is believed to be due to the inability to obtain the accuracy in the pressure and temperature measurements necessary to determine NPSH levels.

As discussed above and shown in Figures 16 and 17, the head rise of the pump was decreasing during the cavitation tests after pump inlet pressure became low enough to allow hydrogen coolant from the bearing cavity to mix with the inlet flow. Although a quantitative effect of the flow mixing on cavitation results is unknown, the coolant flow increases the volume flow and temperature of the hydrogen at the impeller eye, both of which have an adverse effect on cavitation margin. As such, the reported Suction Specific Speeds are believed to be conservative.

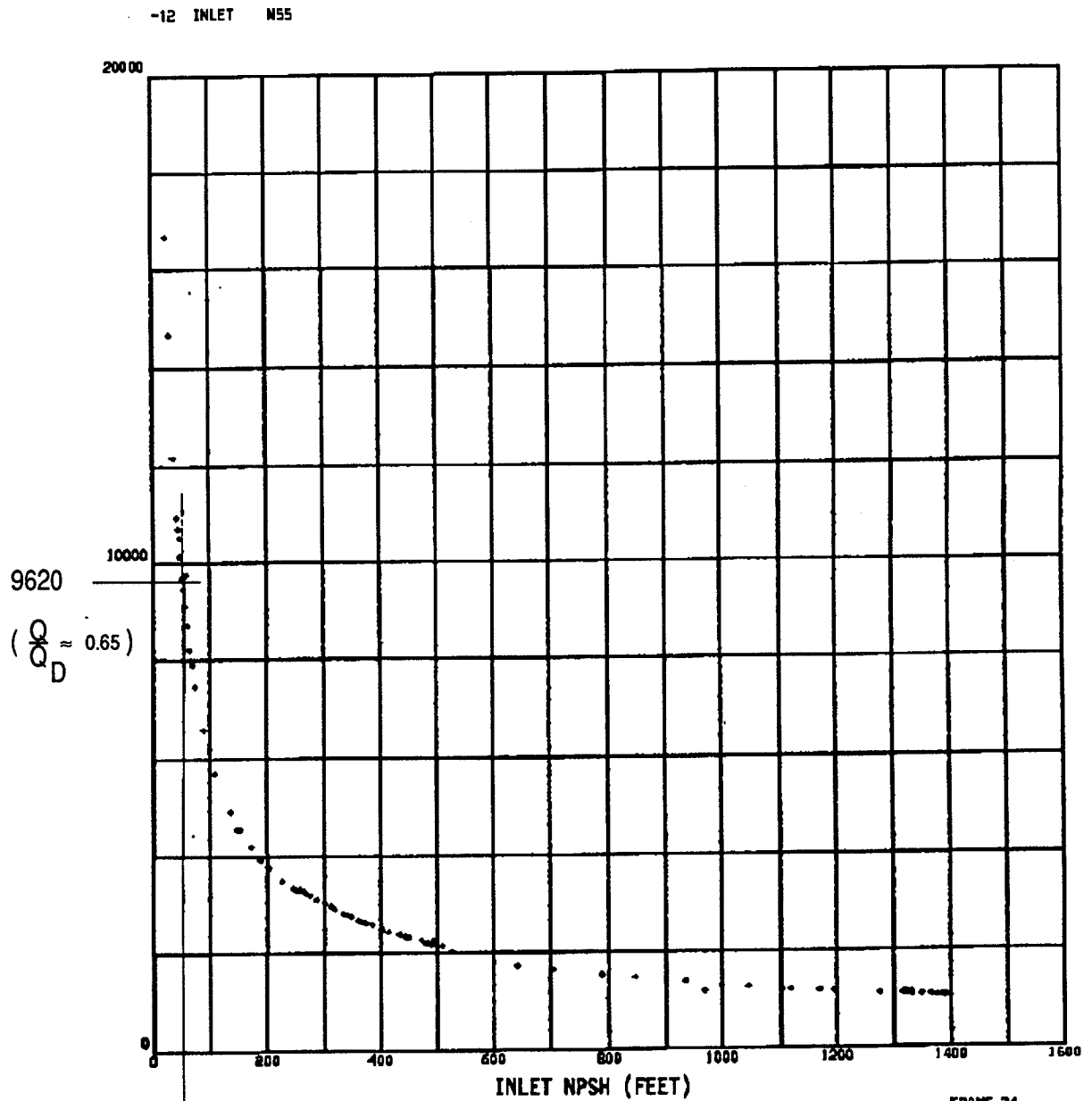
DIFFUSION SYSTEM PERFORMANCE

A cross sectional view of the diffusion system for Configuration 2 is shown in Figure 22. Impeller flow discharges directly into a volute with a diffusing section at the volute exit. Because of the very small size, the volute flow area (for constant velocity) was made oversize by the empirical factor given in Table II. As a result there was recovery of static pressure in both the volute and the volute exit section as shown in Figure 23 for the test at 80 percent design speed. Pump overall static head noted on the figure reflects measurements from a location 20 diameters upstream of the impeller inlet to a location five diameters downstream of the pump discharge. Impeller static head was measured from the same upstream station to the impeller tip. The difference between the two indicates the conversion of impeller exit velocity pressure into static pressure. System performance in hydrogen was similar to water test results, i.e. good static pressure recovery with essentially no change in performance over the range of test flow rate.

HYDRODYNAMIC LOADING

The scope of the program experimental effort included a study of pump axial and radial hydrodynamic loading. Pump internal static pressures were used to determine the pressure distributions on the various pump parts. The pressures acting over a known area are summed up to get the corresponding load. This section presents comparisons of the measured loads in both water and liquid hydrogen.

Figure 18 - Low Thrust Hydrogen Testing
Configuration 2
Cavitation Test 016026, Shaft Speed 61,600 RPM



ADVANCED PROPELLANT TEST FACILITY. TEST 016026.

FRAME 34

NPSH AT 3% HEAD FALLOFF

Figure 19 - Low Thrust Hydrogen Testing
Configuration 2
Cavitation Test 016027, Shaft Speed 61,600 RPM
Suction Specific Speed vs Inlet NPSH

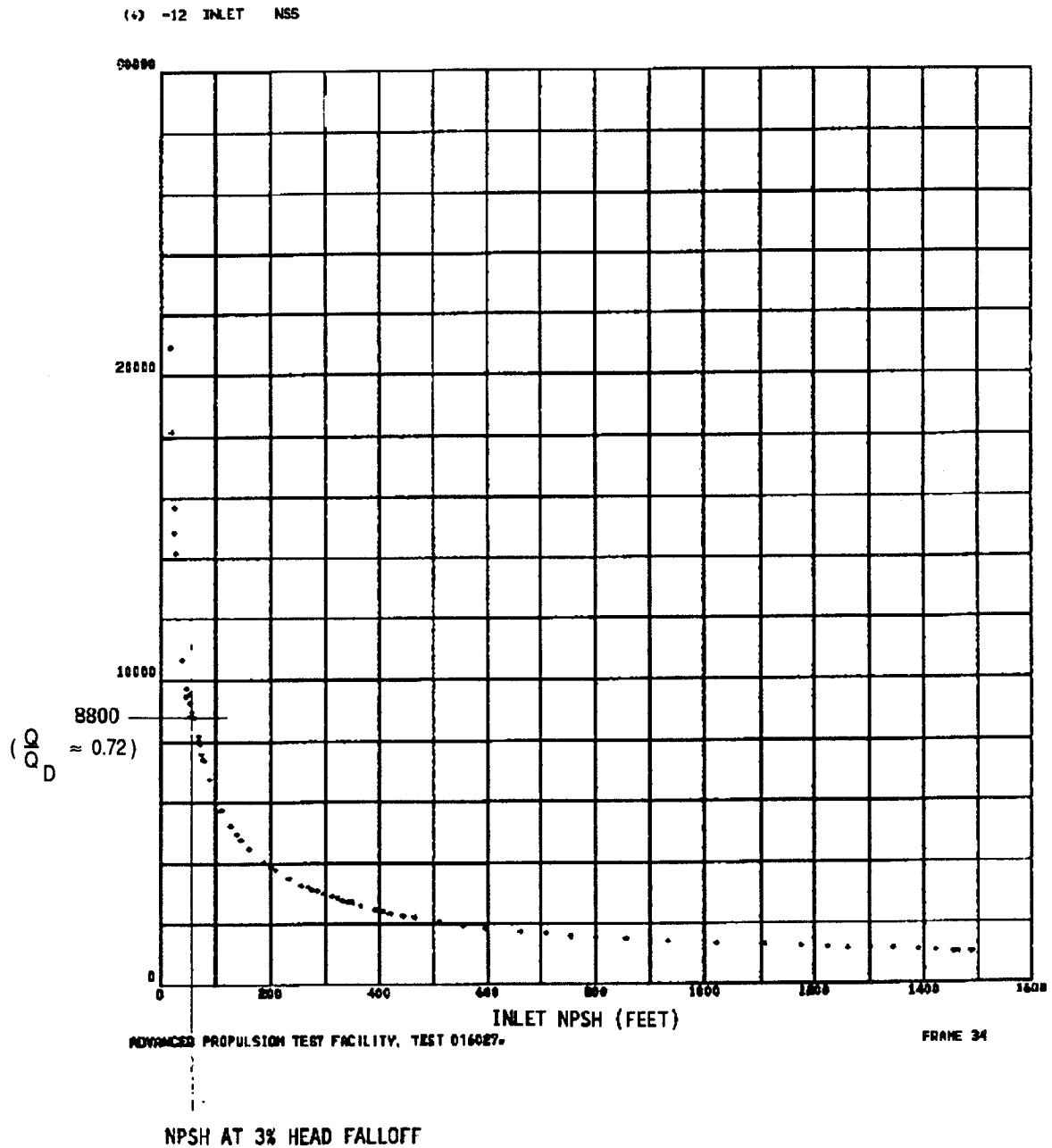


Figure 20 - Low Thrust Hydrogen Testing
Configuration 2
Suction Specific Speed

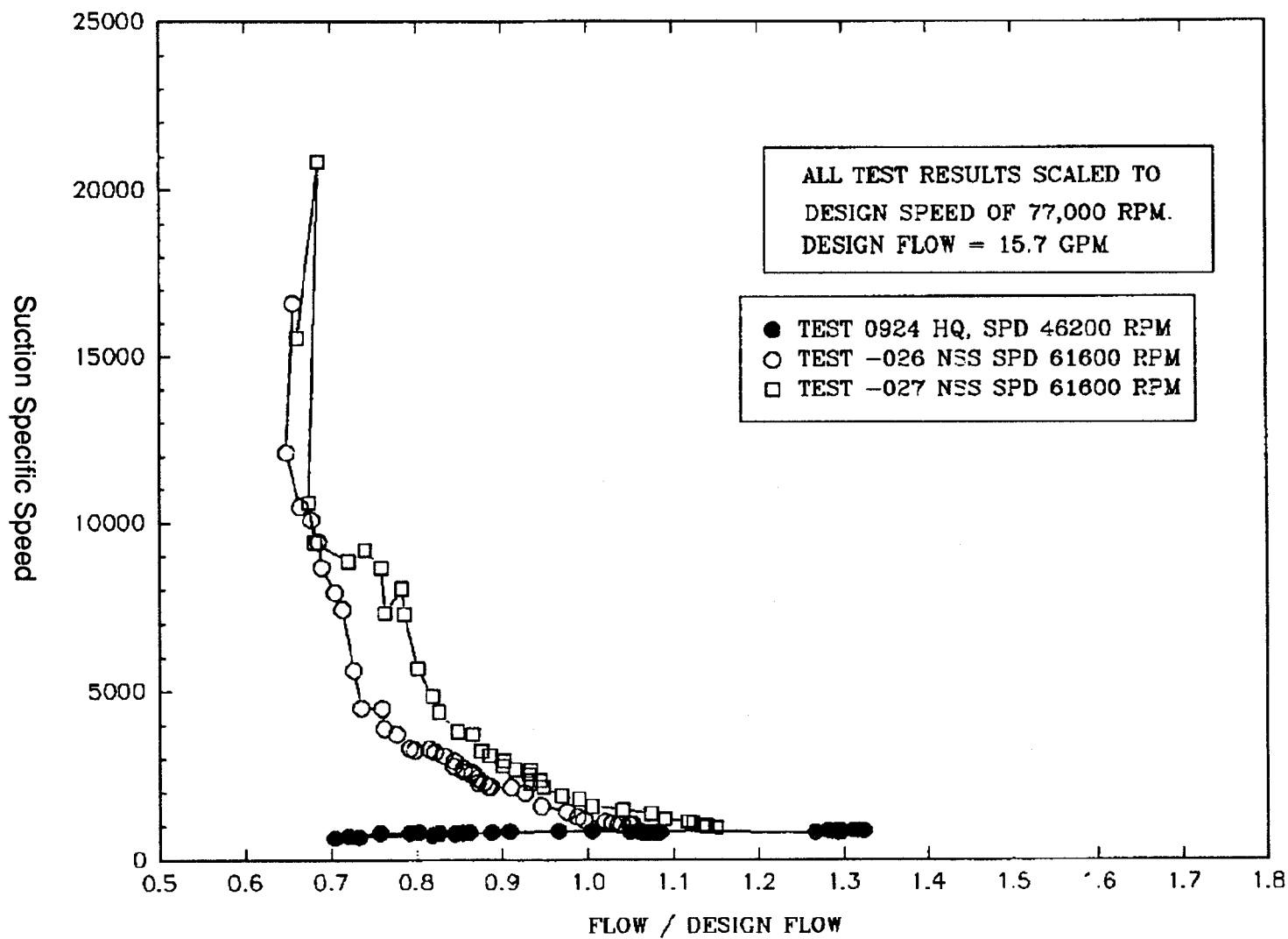


Figure 21 - Low Thrust Hydrogen Testing
Configuration 2
Suction Performance FOR Hydrogen and Water

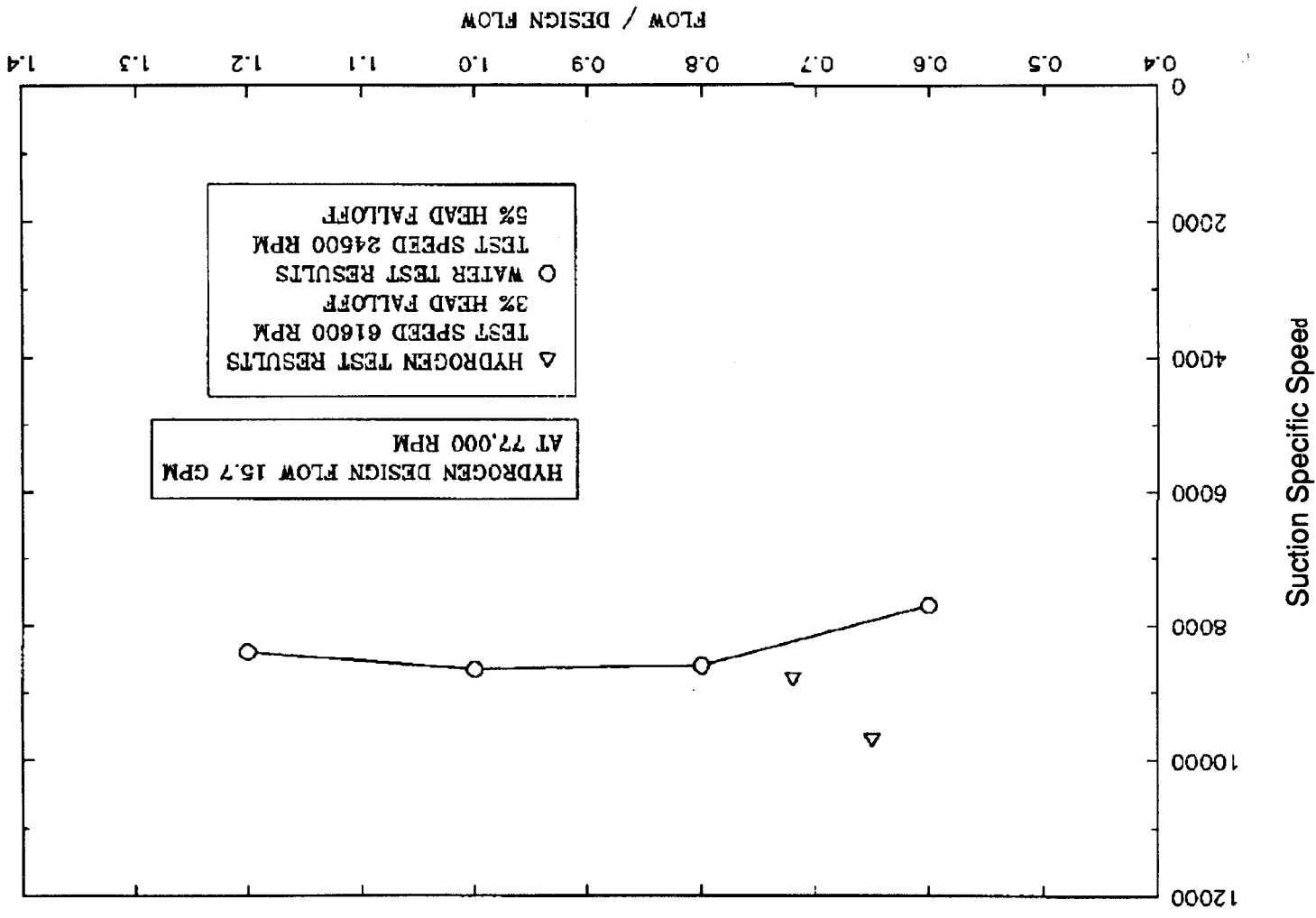
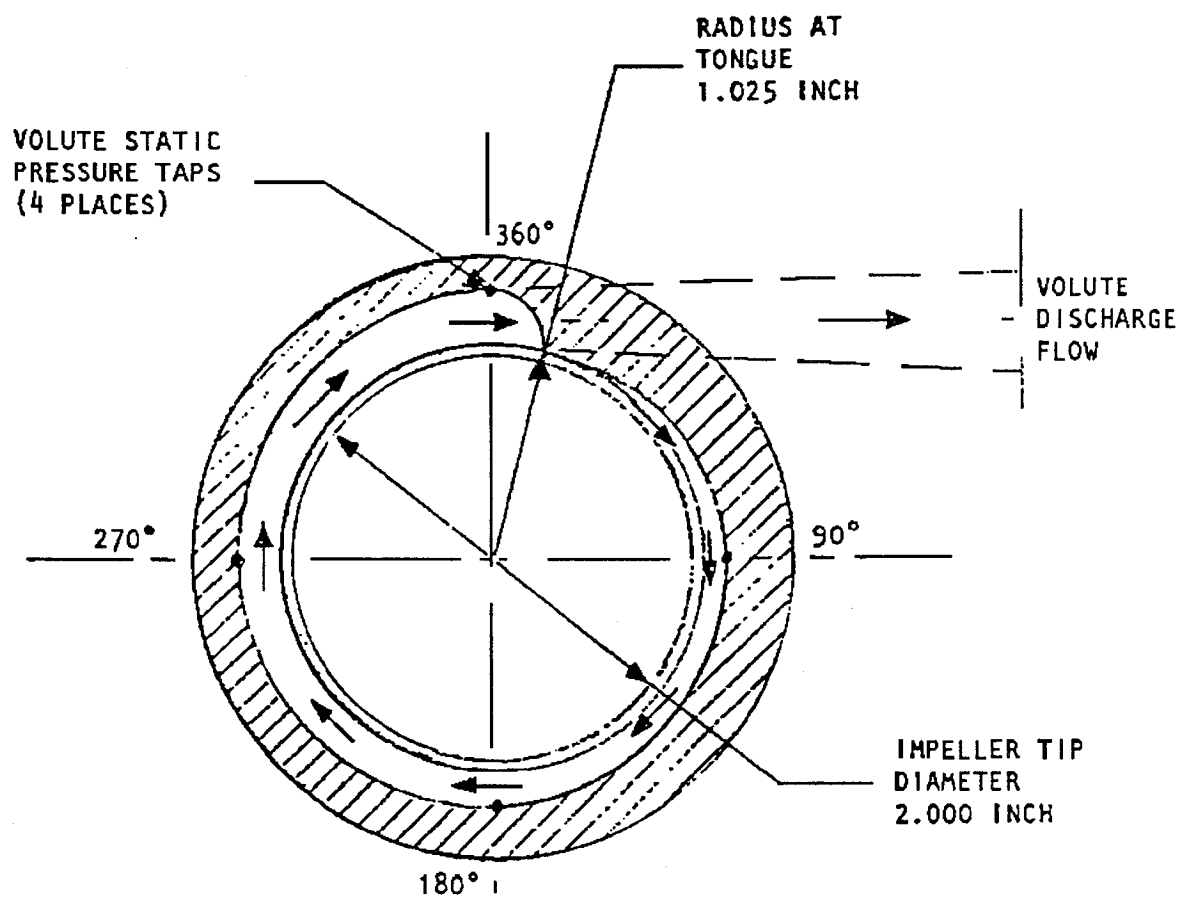


Figure 22 - Diffusion System, Configuration 2



Radial Load The radial load acting on the impeller is determined by integrating the impeller tip static pressure over the circumferential area. The impeller tip pressures were not measured directly, but measurements were made at four equally spaced locations around the outer diameter of the volute (Figure 22). The static pressure at the impeller tip was derived from these four measurements by assuming that the flow from the impeller o.d. to the volute o.d. follows the free vortex relationships.

The static pressure rise to the volute measurement stations were shown in Figure 23. As can be seen, the pressures are increasing with increasing angle. This is a consistent distribution for a volute that is larger in area than required for passing the flow. This distribution will yield a load acting to push the impeller towards the 90 degree side (a pressure distribution that is linear with angle would act exactly towards 90 degrees)

With only four measurements, the accuracy of a calculated angle would not be expected to be very good. The angle calculated was actually between 90 and 180 degrees which is the right general trend. The scaled magnitude of the radial load in hydrogen is shown in Figure 24 based on operation at full speed (77,000 RPM). Also shown are the water test results from reference 1. All three sets of data are seen to be in good agreement when hydrogen results are scaled to consistent conditions. The data show that the volute size is large enough to pass a much larger flow than the pump design flow without introducing significant radial load. This is another reason that small pumps like this should have an oversized volute.

Axial Load The axial load is determined from the measured static pressure distribution on the front and rear impeller face and by the impeller inlet pressure. The front face has three static pressure taps located at the impeller tip, at the wear ring diameter and at a location mid-way between these two. The rear face has two static pressure taps. These are located at the tip and at the wear ring diameter. The fluid pressures in the shroud areas are a function of the effective tangential velocity in the region which is typically defined by a factor K which is the ratio of fluid velocity to wheel speed at any given radius (for the limiting case of pure forced vortex motion $K=1.0$).

The shroud K-factors calculated from the measured static pressures are all higher than expected. The rear shroud K factor averages approximately 0.75 and the front shroud approximately 0.73. From experience on similar small scale turbopumps (MK-51 fuel and oxidizer pumps) the K-factors are characteristically high. A possible explanation is the relatively large impeller tip shroud thickness which increases the tangential velocity of the fluid entering the shroud cavity. Also, the boundary layers on the small size impeller would be larger leading to high tangential velocities, and the wear ring flow is primarily derived from these boundary layer flows.

The axial load at design speed and flow rate on the front and rear shrouds are 570 lb and 552 lb, respectively giving an unbalance of 18 lb. The pump inlet pressure at 80.3 psig adds to the shroud imbalance by a 59 lb load. The remaining loads on the pump and turbine are relatively small compared to these loads. The turbine, operating at full admission, contributes less than one lb axial load. The net axial load of 77 lb is primarily a function of the pump inlet pressure (contributing 77% of the total load).

Figure 23 - Low Thrust Hydrogen Testing
Configuration 2
Pump Impeller, Volute Head vs Flow

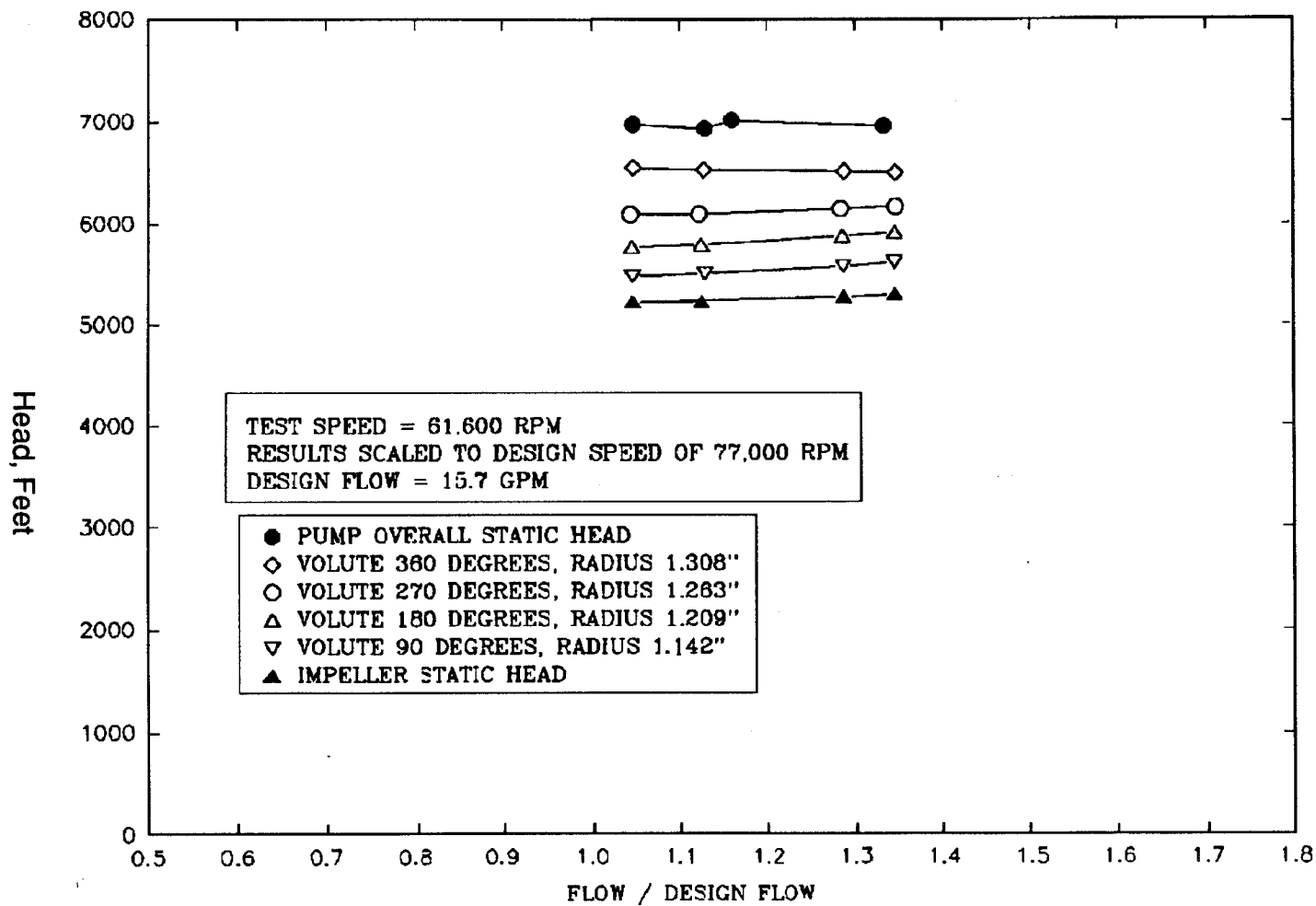
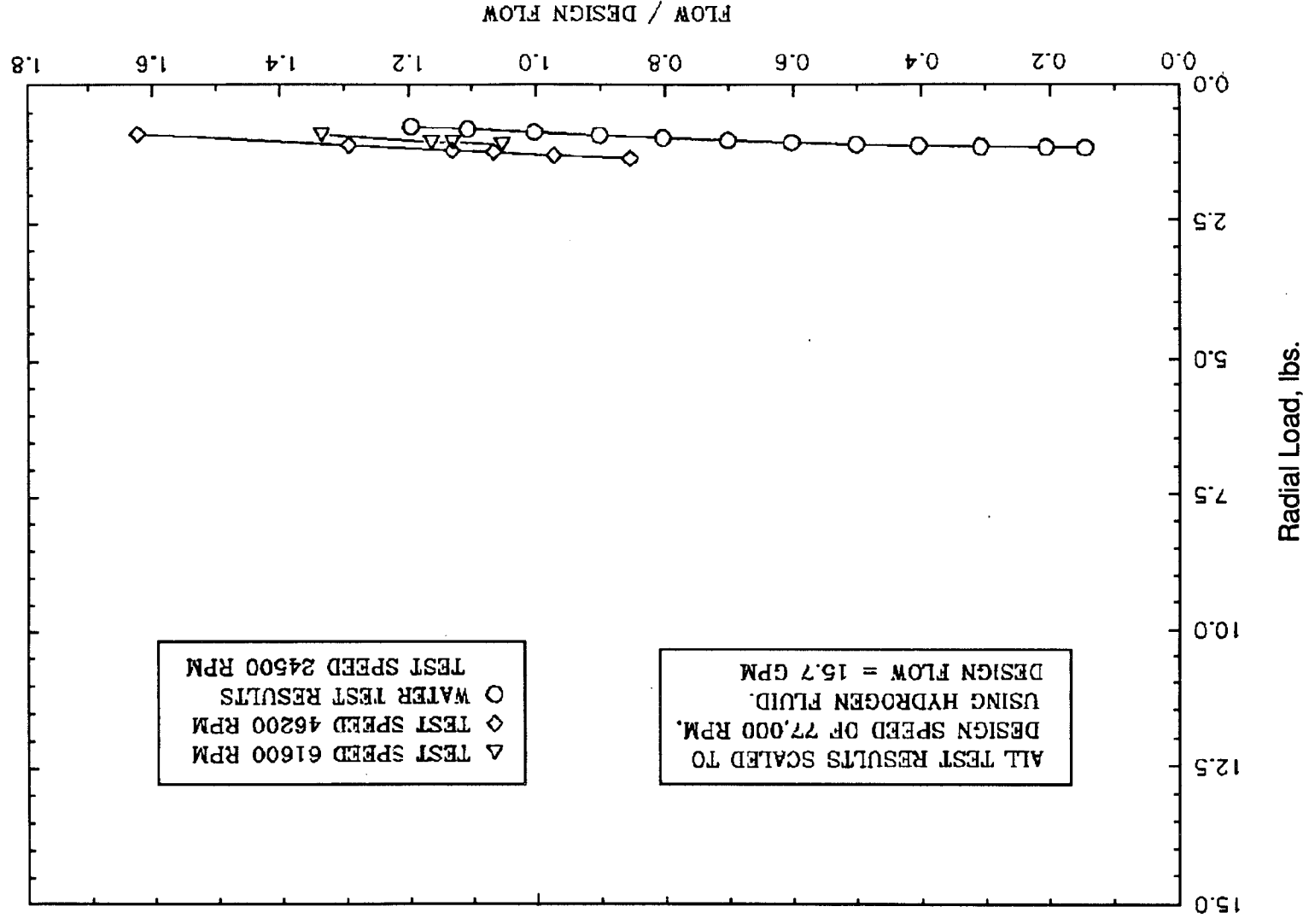


Figure 24 - Low Thrust Hydrogen Testing
Configuration 2 Radial Load



CONCLUDING REMARKS

Testing was successfully completed to evaluate a small, low specific speed centrifugal pump stage in liquid hydrogen. Test speeds were 60% and 80% of the 77,000 RPM design speed. The head/flow characteristic in hydrogen was relatively flat over the test flow range similar to the head/flow characteristic determined in previous water tests. When scaled to design speed, test results at 80% speed show a head rise of 7,000 feet at design flow. Impeller wear ring radial clearances for the hydrogen tests were over two times the design value and significantly affected the test efficiency which was measured at 30.3%. Test efficiency adjusted to reflect a 0.002 inch design clearance is 43.7%. Limited cavitation test data show improved suction performance in hydrogen over the water test cavitation performance.

In general, the hydrogen tests results show that relatively good performance can be achieved for small, low specific speed centrifugal pumps with reasonable control of wear ring clearances.

REFERENCE:

1. Furst, R.B.: Small Centrifugal Pumps for Low-Thrust Rocket Engines - Interim Report. NASA R 174913, Rockwell International, Rocketdyne Division, March 1986.

1. Report No. NASA CR-187117		2. Government Accession No.		3. Recipient's Catalog No.	
4. Title and Subtitle Hydrogen Test of a Small, Low Specific Speed Centrifugal Pump Stage				5. Report Date May 1991	
				6. Performing Organization Code	
7. Author(s) Rocketdyne Engineering				8. Performing Organization Report No. RI/RD 87-164	
				10. Work Unit No. YOS 1449	
9. Performing Organization Name and Address Rocketdyne Division Rockwell International 6633 Canoga Avenue Canoga Park, CA 91304				11. Contract or Grant No. NAS3-23164	
				13. Type of Report and Period Covered Contractor Report Final	
12. Sponsoring Agency Name and Address National Aeronautics and Space Administration Lewis Research Center Cleveland, Ohio 44135-3191				14. Sponsoring Agency Code	
15. Supplementary Notes Project Manager: G. Paul Richter NASA - Lewis Research Center Cleveland, Ohio 44135					
16. Abstract A small, low specific speed (430 RPM*GPM**0.5/FT**0.75) centrifugal pump stage with a 2 inch tip diameter, 0.030 inch tip width shrouded impeller and volute collector was tested with liquid hydrogen as the pumped fluid. The hydrodynamic design of the pump stage is summarized and the noncavitating and cavitating performance results are presented. Test speeds were 60% and 80% of the 77,000 RPM design speed. Liquid hydrogen test results are compared with data from previous tests of the stage in water.					
17. Key Words (Suggested by Author(s)) Low-Thrust Rocket Engine Pumps Low Specific Speed Pumps Centrifugal Pumps Hydrogen Pumps				18. Distribution Statement Unclassified - Unlimited Subject Category - 20	
19. Security Classif. (of this report) Unclassified		20. Security Classif. (of this page) Unclassified		22. Price* A03	
				21. No. of pages 46	